WESTERDIJK FUNGAL BIO DIVERSITY INSTITUTE

Re-examination of species limits in *Aspergillus* section *Flavipedes* using advanced species delimitation methods and description of four new species

F. Sklenář[1,2], Ž. Jurjević[3], J. Houbraken[4], M. Kolařík[1,2], M.C. Arendrup[5,6,7], K.M. Jørgensen[5], J.P.Z. Siqueira[8,9], J. Gené[9], T. Yaguchi[10], C.N. Ezekiel[11], C. Silva Pereira[12], and V. Hubka[1,2,10*]

[1]*Department of Botany, Faculty of Science, Charles University, Prague, Czech Republic;* [2]*Laboratory of Fungal Genetics and Metabolism, Institute of Microbiology, Czech Academy of Sciences, Prague, Czech Republic;* [3]*EMSL Analytical, Cinnaminson, NJ, USA;* [4]*Westerdijk Fungal Biodiversity Institute, Utrecht, the Netherlands;* [5]*Unit of Mycology, Statens Serum Institut, Copenhagen, Denmark;* [6]*Department of Clinical Microbiology, Rigshospitalet, Copenhagen, Denmark;* [7]*Department of Clinical Medicine, University of Copenhagen, Copenhagen, Denmark;* [8]*Laboratório de Microbiologia, Faculdade de Medicina de São José do Rio Preto, São José do Rio Preto, Brazil;* [9]*Unitat de Micologia, Facultat de Medicina i Ciències de la Salut, IISPV, Universitat Rovira i Virgili, Reus, Spain;* [10]*Medical Mycology Research Center, Chiba University, Chuo-ku, Chiba, Japan;* [11]*Department of Microbiology, Babcock University, Ilishan Remo, Ogun State, Nigeria;* [12]*Instituto de Tecnologia Química e Biológica António Xavier, Universidade Nova de Lisboa (ITQB NOVA), Oeiras, Portugal*

**Correspondence*: V. Hubka, vit.hubka@gmail.com, hubka@biomed.cas.cz

Abstract: Since the last revision in 2015, the taxonomy of section *Flavipedes* evolved rapidly along with the availability of new species delimitation techniques. This study aims to re-evaluate the species boundaries of section *Flavipedes* members using modern delimitation methods applied to an extended set of strains (n = 90) collected from various environments. The analysis used DNA sequences of three house-keeping genes (*benA*, *CaM*, *RPB2*) and consisted of two steps: application of several single-locus (GMYC, bGMYC, PTP, bPTP) and multi-locus (STACEY) species delimitation methods to sort the isolates into putative species, which were subsequently validated using DELINEATE software that was applied for the first time in fungal taxonomy. As a result, four new species are introduced, *i.e. A. alboluteus*, *A. alboviridis*, *A. inusitatus* and *A. lanuginosus*, and *A. capensis* is synonymized with *A. iizukae*. Phenotypic analyses were performed for the new species and their relatives, and the results showed that the growth parameters at different temperatures and colonies characteristics were useful for differentiation of these taxa. The revised section harbors 18 species, most of them are known from soil. However, the most common species from the section are ecologically diverse, occurring in the indoor environment (six species), clinical samples (five species), food and feed (four species), droppings (four species) and other less common substrates/environments. Due to the occurrence of section *Flavipedes* species in the clinical material/hospital environment, we also evaluated the susceptibility of 67 strains to six antifungals (amphotericin B, itraconazole, posaconazole, voriconazole, isavuconazole, terbinafine) using the reference EUCAST method. These results showed some potentially clinically relevant differences in susceptibility between species. For example, MICs higher than those observed for *A. fumigatus* wild-type were found for both triazoles and amphotericin B for *A. ardalensis, A. iizukae,* and *A. spelaeus* whereas *A. lanuginosus, A. luppiae, A. movilensis, A. neoflavipes, A. olivimuriae* and *A. suttoniae* were comparable to or more susceptible as *A. fumigatus*. Finally, terbinafine was *in vitro* active against all species except *A. alboviridis*.

Key words: *Aspergillus flavipes*, Antifungal susceptibility testing, Clinical fungi, Indoor fungi, Multigene phylogeny, Soil-borne fungi, Species delimitation.
Taxonomic novelties: New species: *Aspergillus alboluteus* F. Sklenar, Jurjević, Ezekiel, Houbraken & Hubka, *Aspergillus alboviridis* J.P.Z. Siqueira, Gené, F. Sklenar & Hubka, *Aspergillus inusitatus* F. Sklenar, C. Silva Pereira, Houbraken & Hubka, *Aspergillus lanuginosus* F. Sklenar & Hubka.

Available online 16 December 2021; https://doi.org/10.1016/j.simyco.2021.100120.

INTRODUCTION

Aspergillus is a large genus of filamentous fungi, which currently contains 446 accepted species and this number is rapidly rising. Aspergilli have traditionally been classified into subgenera and sections, and this classification has been recently revised and updated with the addition of series rank (Houbraken *et al.* 2020). According to this most up-to-date overview, the accepted species are distributed over six subgenera, 27 sections, and 75 series. Thom & Church (1926) introduced the *A. flavipes* group and section *Flavipedes* was formally established by Gams *et al.* (1985). The section is close to sections *Terrei* and *Jani* (Kocsubé *et al.* 2016) and is subdivided in four series: *Flavipedes*, *Neonivei*, *Olivimuriarum* and *Spelaei* (Houbraken *et al.* 2020). Phylogenetic analysis performed by Peterson (2008) demonstrated the presence of undescribed species diversity and the need for a proper taxonomic revision. The section was revised by Hubka *et al.* (2015), who accepted 10 species, two of which, *A. frequens* and *A. mangaliensis*, are synonymous to *A. micronesiensis* and *A. templicola*, published independently during the same period (Visagie *et al.* 2014, Arzanlou *et al.* 2016). In addition, Visagie *et al.* (2014) introduced another species, *A. capensis*, a close relative of *A. iizukae*, isolated from house dust. Another four species were described since then, namely, *A. urmiensis* described from hypersaline soils in Iran (Arzanlou *et al.* 2016), *A. suttoniae* from human sputum in the USA (Siqueira *et al.* 2018), *A. olivimuriae* from olive brine in Italy (Crognale *et al.* 2019) and *A. sakultaensis* from a water sample collected in Egypt (Zohri & Al-Bedak 2020). However, the last mentioned species was not validly described [Art. 40.8, Shenzen Code], and the study does not contain sufficient data to clearly classify *A. sakultaensis* into the current system. The isolate was not available for this study, but the DNA sequence of the internal transcribed spacer (ITS) generated by the authors was identical with some strains of *A. templicola*.

Peer review under responsibility of Westerdijk Fungal Biodiversity Institute.

Studies in Mycology

The species from section *Flavipedes* occur globally in soil (Klich 2002) and they can also grow as endophytes (El-Elimat *et al.* 2014), cause food spoilage (Pitt & Hocking 2009), or contaminate the indoor environment (Visagie *et al.* 2014). They are also occasionally isolated from clinical samples and infrequently cause opportunistic human or animal infections (Schultz *et al.* 2008, Gehlot *et al.* 2011, Siqueira *et al.* 2018). Representatives of section *Flavipedes* are able to produce a wide range of metabolites, summarized by Frisvad & Larsen (2015). These include mycotoxins such as sterigmatocystin (Tuomi *et al.* 2000) and citrinin (Greenhill *et al.* 2008), or pharmaceutical drugs (established or potential) such as HMG CoA reductase inhibitor lovastatin (Valera *et al.* 2005) and antiviral xanthones (Kang *et al.* 2018). Section *Flavipedes* species are also studied for their biotechnological potential and various biological activities. For example, *A. flavipes* possesses the potential to act as a biocontrol agent (El-Sayed & Ali 2020), *A. polyporicola* and *A. spelaeus* may be employed in the remediation of crude oil contaminated soil (Al-Dhabaan 2021) and *A. iizukae* produces oxidative enzymes with an industrial application (Noman *et al.* 2020).

In this study, we assembled a dataset of 90 strains belonging to section *Flavipedes*, which were newly isolated or originated from previous studies. We re-examined species boundaries of currently known species using modern species delimitation methods and discovered several new ones. The species delimitation and phylogenetic analyses utilized the DNA sequence data of three house-keeping genes. Phenotypic variability was examined in the species related to the newly discovered ones in order to find additional support for species hypotheses. The methodology of the species delimitation analysis follows up on previous studies within the genus *Aspergillus* (Sklenář *et al.* 2017, 2020, Hubka *et al.* 2018a, 2018b) with notable changes in the species validation step, where we used a newly developed program DELINEATE as opposed to utilization of BPP (Bayesian Phylogenetics and Phylogeography) (Yang 2015) in previous studies.

MATERIALS AND METHODS

Strains

The newly isolated strains obtained from the indoor environment were isolated as described previously (Jurjević *et al.* 2015) and the remaining strains were mostly obtained from collaborators or culture collections. Detailed information about provenance of the strains is listed in Table 1. Dried holotype and isotype specimens of the newly described species were deposited into the herbarium of the Mycological Department, National Museum, Prague, Czech Republic (PRM) and/or into the herbarium at the Westerdijk Fungal Biodiversity Institute (CBS H; Utrecht, the Netherlands). Nomenclatural novelties and descriptions were deposited in MycoBank (Crous *et al.* 2004).

Molecular studies

Total genomic DNA was isolated from 7-d-old cultures with ArchivePure DNAyeast (5 PRIME Inc., Gaithersburg, MD, USA) or NucleoSpin® Soil (Macherey–Nagel, Düren, Germany) isolation kits. The quality of the isolated DNA was verified using a NanoDrop 1 000 Spectrophotometer.

The ITS region of rDNA was amplified using forward primer ITS1 (White *et al.* 1990) and reverse primers NL4 (O'Donnell 1993) or ITS4 (White *et al.* 1990), a part of the β-tubulin gene (*benA*) was amplified using forward primers Bt2a (Glass & Donaldson 1995), T10 (O'Donnell & Cigelnik 1997) or Ben2f (Hubka & Kolařík 2012) and reverse primer Bt2b (Glass & Donaldson 1995), a part of the calmodulin gene (*CaM*) was amplified using forward primers CF1L, CF1M (Peterson 2008) or cmd5 (Hong *et al.* 2006) and reverse primers CF4 (Peterson 2008) or cmd6 (Hong *et al.* 2006) and a part of the RNA polymerase II second largest subunit gene (*RPB2*) was amplified using forward primer fRPB2-5F and reverse primer fRPB2-7CR (Liu *et al.* 1999). Various primer pairs were used for the amplification of ITS, *benA* and *CaM* loci because the sequences were generated across various research groups. Thus, it was not due to the failure of PCR with some primer combinations.

The PCR reaction volume of 25 µL contained 1.2 µL (10-20 ng) of DNA, 1 µL of both primers (10 µM), 0.25 µL of DreamTaq DNA Polymerase (Thermo Scientific, Waltham, MA) and 2.5 µl of DreamTaq PCR buffer and 2.5 µl of dNTP. The ITS rDNA, *benA* and *CaM* fragments were amplified using following thermal cycle profile: 93 °C/2 min; 30 cycles of 93 °C/30 s; 55 °C/30 s; 72 °C/60 s; 72 °C/10 min. Partial *RPB2* gene fragments were amplified using above-mentioned cycle or touchdown thermal-cycling: 93 °C/2 min; 5 cycles of 93 °C/30 s, 65–60 °C/30 s, 72 °C/60 s; 38 cycles of 93 °C/30 s, 55 °C/30 s, 72 °C/60 s; 72 °C/10 min. PCR products were purified with ethanol and sodium acetate in a 96-well plate; 2 µL of 3 M NaOAc and 60 µL of 96 % EtOH was mixed with 20 µL of PCR product. The plate was sealed, twisted several times and incubated in the refrigerator for 20 min. After incubation, the plate was centrifuged for 30 min at 4 °C and 3 000 rpm, the supernatant was removed and 85 µL 70 % EtOH was added. The plate was centrifuged for 15 min at 4 °C and 3 000 rpm, the supernatant was subsequently removed, the pellet was dried at room temperature for 20 min and resuspended in 10 µL of H_2O.

Newly obtained DNA sequences were inspected in FinchTV v. 1.4 (available online https://digitalworldbiology.com/FinchTV) and assembled in Bioedit v. 7.0.5 (Hall 1999). Multiple sequence alignments were created in MAFFT v. 7 (Katoh & Standley 2013) using the G-INS-I strategy. Sequences were deposited into GenBank with accession numbers shown in Table 1. All alignments are available from the Dryad Digital Repository: https://doi.org/10.5061/dryad.dz08kprxj.

Phylogenetic analysis and species delimitation

In order to demonstrate the phylogenetic relationships within section *Flavipedes*, we calculated a Maximum Likelihood (ML) tree in IQ-TREE v. 2.0 (Nguyen *et al.* 2015) using a concatenated alignment of all four loci as input. The inference was setup as partitioned analysis and the best-fitting model for each locus was determined using the Bayesian information criterion (BIC) in jModelTest v. 2.1.7 (Posada 2008). Selected models are listed in Table 2 together with the respective alignment statistics. To determine the branch support, the analysis ran for 1 000 bootstrap replicates.

For the purpose of species delimitation analyses, the dataset was split into two parts corresponding to series *Flavipedes* and *Spelaei* as designated by Houbraken *et al.* (2020). Series *Neonivei* and *Olivimuriarum* were excluded as these are single

Table 1. *Aspergillus* strains from section *Flavipedes* examined in this study.

Species	Strain numbers[1]	Provenance (substrate, locality, year of isolation, collector/isolator)	GenBank/EMBL accession numbers[2]			
			ITS rDNA	*benA*	*CaM*	*RPB2*
A. alboluteus	CBS 145855^T = CCF 5695^T = EMSL 2420^T = IFM 66815^T	USA, Pennsylvania, Philadelphia, outdoor air, 2014, Ž. Jurjević	**MW448663**	**MW478497**	**MW478511**	**MW478532**
	CBS 145859 = CCF 6201 = EMSL 3060	USA, Florida, Seminole, A/C Vent – swab, 2015, Ž. Jurjević	**MW448662**	**MW478496**	**MW478510**	**MW478531**
	CBS 145854 = CCF 4916 = EMSL 2311 = IFM 66816	USA, California, indoor air, 2005, Ž. Jurjević	**MW448664**	**MW478498**	**MW478512**	**MW478533**
	CCF 5849 = EMSL 2446 = IFM 66817	USA, Tennessee, Jackson, storage room - swab, 2014, Ž. Jurjević	**MW448665**	**MW478499**	**MW478513**	**MW478534**
	DTO 410-I8 = CBS 147065 = CCF 6551	Nigeria, Abia, Isiala Ngwa South, Obuba, multicrop farm, C.N. Ezekiel	**MW448666**	**MW478500**	**MW478514**	**MW478535**
A. alboviridis	CBS 142665^T = FMR 15175^T = CCF 6049^T = IFM 66819^T	Spain, Balearic Islands, Mallorca, Pollença, herbivore dung, 2016, J. Gené & J.P.Z. Siqueira	LT798909	LT798936	LT798937	LT798938
A. ardalensis	NRRL 62824^T = CCF 4031^T = CCF 4426^T = CMF ISB 1688^T = CBS 134372^T	Spain, Andalucia, Ardales, near Cueva de Doña Trinidad, soil, 2008, A. Nováková	FR733808	HG916683	HG916725	HG916704
	IHEM 17781	France, Giens, hospital environment, 2000, J.-Ph. Bouchara	**MW448667**	**LN909026**	**MW478515**	**MW478536**
A. flavipes	NRRL 302^T = CCF 3067^T = IMI 171885^T = ATCC 24487^T = FRR 0302^T	Received by Charles Thom in 1922 from Da Fonseca as Bainier's culture of *Sterigmatocystus flavipes*	EF669591	EU014085	EF669549	EF669633
	NRRL 4852 = IMI 345934 = CCF 4836 (ex-type of *A. archiflavipes*)	Uruguay, dead beetle, received in NRRL from CBS as Blochwitz's strain of *A. archiflavipes*, W. Herter	LM999909	LM644261	LM644241	LM644260
A. iizukae	NRRL 3750^T = CBS 541.69^T = IMI 141552^T = CCF 4548^T	Japan, Gymna Prefecture, Fujioka, soil from stratigraphic drilling core, 1969, J. Sugiyama	EF669597	EU014086	EF669555	EF669639
	CBS 138188^T = DTO 179-E6^T (ex-type of *A. capensis*)	South Africa, Cape Town, house dust, 2010, E. Whitfield & K. Mwange	KJ775550	KJ775072	KJ775279	KP987020
	CanS-34A	China, Wuhan, oilseed rape (*Brassica napus*), between 2008-2010	MK072769	MK215220	MK215219	MK215221
	CCF 1895	Czechia, Most (brown lignite district), soil of spoil bank, 1984, M. Černý	FR727134	FR775336	HG916728	HG916707
	CCF 4033 = CMF ISB 1551 = NA16 = Y14	Czechia, Most (brown lignite district), soil of spoil bank tip, 2004, A. Nováková	FR733809	HG916686	HG916729	**MW478537**
	CCF 4032 = CMF ISB 1245	Germany, Weissagker Berg near Cottbus, Lusatian brown lignite district, soil of spoil bank, 1999, A. Nováková	HG915894	HG916687	HG916730	HG916708
	CMF ISB 2544	Romania, Dobrogea, Mangalia, soil near Movile Cave, 2011, A. Nováková	HG915895	HG916694	HG916731	HG916709
	CMF ISB 2417	Romania, National Park Apuseni Mountains, Meziad Cave, earthworm casts, 2009, A. Nováková	HG915896	HG916688	HG916732	HG916710
	CMF ISB 2616	Czechia, Ječmeniště, National Nature Monument, soil, 2012, A. Nováková	HG915899	HG916689	HG916733	HG916711
	CMF ISB 2617	Czechia, Kolby, National Reservation Pouzdřanská step, soil, 2012, A. Nováková	HG915897	HG916692	HG916734	HG916712
	CMF ISB 2618	Czechia, Kolby, National Reservation Pouzdřanská step, soil, 2012, A. Nováková	HG915898	HG916693	HG916735	HG916713
	CMF ISB 2619		HG915900	HG916690	HG916736	HG916714

(*continued on next page*)

Table 1. (Continued).

Species	Strain numbers[1]	Provenance (substrate, locality, year of isolation, collector/isolator)	GenBank/EMBL accession numbers[2]			
			ITS rDNA	*benA*	*CaM*	*RPB2*
		Czechia, Kolby, National Reservation Pouzdřanská step, earthworm casts, 2012, A. Nováková				
	CMF ISB 2620	Czechia, Kolby, National Reservation Pouzdřanská step, earthworm casts, 2012, A. Nováková	HG915901	HG916691	HG916737	HG916715
	NRRL 58963 = CCF 4843 = ZJ 1256	USA, Illinois, indoor air of a home, 2009, Ž. Jurjević	LM644237	LM644268	LM644245	**MW478538**
	CCF 4844 = ZJ 1817	USA, Idaho, Boise, indoor air of a home, 2012, Ž. Jurjević	LM644238	LM644269	LM644244	**MW478539**
	CCF 4845 = S746	Romania, Movile Cave, cave sediment, 2013, A. Nováková	LM999906	LM644270	LM644243	**MW478540**
	UTHSCSA DI14-219	USA, Illinois, human, bronchoalveolar lavage, 2012, D. Sutton	LT899477	LT899528	LT899579	LT899634
	FMR 15051	Spain, Catalonia, Els Ports Natural Park, herbivore dung, 2016, J. Gené	LT899475	LT798968	LT899577	LT899632
	FMR 15606	Spain, Catalonia, Els Ports Natural Park, herbivore dung, 2016, J. Gené	LT899476	LT798969	LT899578	LT899633
	CCF 5786 = EMSL 3408	USA, Florida, Saint Petersburg, bedroom floor – swab, 2016, Ž. Jurjević	**MW448668**	**MW478501**	**MW478516**	**MW478541**
A. inusitatus	DTO 121-G5^T = CBS 147044^T = CCF 6552^T	Tunisia, Ras Rajel, soil in oak forest, 2009, C. Silva Pereira	**MW448669**	**MW478502**	**MW478517**	**MW478542**
A. lanuginosus	NRRL 4610^T = IMI 350352^T = CCF 4551^T = IFM 66818^T	Haiti, Fonds Parisien, soil	EF669604	EU014080	EF669562	EF669646
A. luppiae	NRRL 6326^T = CBS 653.74^T = CCF 4545^T	France, Provence, near Aups, natural truffle soil, 1972, A.M. Luppi-Mosca	EF669617	EU014079	EF669575	EF669659
A. micronesiensis	CBS 138183^T = DTO 267-D5^T	Federated States of Micronesia, Yela of Kosrae Island, house dust, 2010, E. Whitfield & K. Mwange	KJ775548	KJ775085	KP987067	KP987023
	NRRL 4578 = ATCC 16805 = CBS 586.65 = IMI 135423 = CCF 4555 (ex-type of *A. frequens*)	Haiti, soil, 1960, J. Rabel	EF669602	EU014082	EF669560	EF669644
	CCF 2026	Czechia, Prague, archive material, 1986, O. Fassatiová	HG915893	HG916684	HG916726	HG916705
	NRRL 295 = ATCC 16814 = CBS 585.65 = IMI 135422 = CCF 4554 = FRR 0295	USA, Minnesota, dairy products, 1933, H. Macy	EF669588	EU014081	EF669546	EF669630
	CCF 4005	Czechia, Hradec Králové, hospital indoor air, 2005, V. Buchta	FR727135	HG916685	HG916727	HG916706
	NRRL 4263 = CCF 4556	India, Dehradun New Forest, soil, 1955, K.B. Bakshi	EF669600	EU014083	EF669558	EF669642
	NRRL 286 = ATCC 1030 = FRR 0286	Received in NNRL from Dr. J. Westerdijk (CBS)	AY373849	LM644262	LM644246	LM644258
	NRRL 26246 = CCF 4838	China, soil, 1944	LM999905	LM644263	LM644247	LM644257
	NRRL 58660 = CCF 4839 = ZJ 1111	Trinidad & Tobago, indoor air of a home, 2009, Ž. Jurjević	LM644239	LM644264	LM644248	**MW478543**
	NRRL 58682 = CCF 4840 = ZJ 1132	Puerto Rico, indoor air of a home, 2009, Ž. Jurjević	LM644240	LM644265	LM644251	**MW478544**
	NRRL 58899 = CCF 4841 = ZJ 1267	USA, New York, indoor air of a home, 2009, Ž. Jurjević	LM999903	LM644266	LM644249	**MW478545**
	NRRL 58598 = CCF 4842 = ZJ 1038	USA, New Jersey, indoor air of a home, 2008, Ž. Jurjević	LM999904	LM644267	LM644250	**MW478546**
	IHEM 18446	Belgium, Brussels, floor in hospital, 2001, BCCM/IHEM collection	**MW448670**	**LN909029**	**MW478518**	**MW478547**
	IHEM 662	Belgium, Brussels, indoor air in hospital, 1980, BCCM/IHEM collection	**MW448671**	**LN909030**	**MW478519**	**MW478548**
	IHEM 22506 = RV 21840	Belgium, Liège, human lung, 1967, University Hospital Liège	**MW448672**	**LN909028**	**MW478521**	**MW478549**

Table 1. (Continued).

Species	Strain numbers[1]	Provenance (substrate, locality, year of isolation, collector/isolator)	GenBank/EMBL accession numbers[2]			
			ITS rDNA	*benA*	*CaM*	*RPB2*
	IHEM 22505 = RV 42608	Belgium, Antwerp, human sputum (male), 1979, D. Van Vijver	**MW448673**	**LN909027**	**MW478520**	**MW478550**
	CBS 147045 = DTO 247-H3	Mexico, Sayulita, hotel room, house dust, 2009, A. Amend & E. Whitfield & K. Mwange	KP987079	KP987047	KP987062	KP987036
	IMI 357699 = DTO 305-B6 = IBT 23707 (ex-type of *A. sunderbanii nom. inval.*)	India, West Bengal, soil	KP987084	KP987052	KP987069	KP987026
	UTHSCSA DI14-214	USA, California, canine urine, 2012, D. Sutton	LT899480	LT899529	LT899582	LT899637
	FMR 15737	Spain, Canary Islands, Tenerife, 2016, J. Gené	LT899479	LT798971	LT899581	LT899636
A. movilensis	NRRL 62819^T = CCF 4410^T = CMF ISB 2614^T = CBS 134395^T	Romania, Mangalia, Dobrogea, soil near Movile Cave, 2011, A. Nováková	HG915904	HG916697	HG916740	HG916718
	CBS 139559 = CCTU 749 = DTO 203-C9 = IBT 32594	Iran, Urmia, Kabodan Island, soil, between 2011 and 2012, U. Ghosta & R. Samadi	KP987075	KP987043	KP987058	KP987032
	CBS 139562 = CCTU 788 = DTO 203-H3	Iran, Urmia, Kabodan Island, soil, between 2011 and 2012, U. Ghosta & R. Samadi	KP987078	KP987046	KP987061	KP987035
	S1040	Romania, soil above the Movile cave, 2014, A. Nováková	**MW448674**	**MW478503**	**MW478522**	**MW478551**
A. neoflavipes	NNRL 5504^T = ATCC 24484^T = CBS 260.73^T = IMI 171883^T = IFM 40894^T = CCF 4552^T	Thailand, Pak Thong Chai, cellulosic material buried in forest soil, 1968, C. Klinsukont	EF669614	EU014084	EF669572	EF669656
A. olivimuriae	NRRL 66783^T = CCF 6208^T	Italy, Viterbo, olive curing brine, 2012, S. Crognale	MH298877	MH492010	MH492011	MH492012
A. polyporicola	NRRL 32683^T = CCF 4553^T	USA, Hawaii, Hilo, Alien Wet Forest Zoo, basidioma of *Earliella scabrosa* (*Polyporales*), 2003, D.T. Wicklow	EF669595	EU014088	EF669553	EF669637
	NRRL 58570 = CCF 4828	USA, Hawaii, Alien Wet Forest, basidioma of *Rigidoporus microporus* (*Polyporales*), 2003, D.T. Wicklow	HQ288052	LM644274	LM644252	LM644254
	CCF 5427 = EMSL 2612	USA, New York, Holbrook, bedroom - settle plates, 2014, Ž. Jurjević	**MW448675**	**MW478504**	**MW478523**	**MW478552**
	CCF 6262 = EMSL 3169	USA, crawled space - settle plates, 2015, Ž. Jurjević	**MW448676**	**MW478505**	**MW478524**	**MW478553**
A. spelaeus	NRRL 62826^T = CCF 4425^T = CMF ISB 2615^T = CBS 134371^T	Spain, Andalusia, Nerja Cave, cave sediment, 2011, A. Nováková	HG915905	HG916698	HG916741	HG916719
	NRRL 62827 = CCF 544	Czechia, Bohemian Karst, Doutnáč hill near Srbsko, soil, 1961, O. Fassatiová	HG915906	HG916699	HG916742	HG916720
	CCF 4699 = CMF ISB 2659	Czechia, Hostěradice, National Nature Monument U Kapličky, *Allolobophora hrabei* intestine, 2012, A. Nováková	HG915907	HG916700	HG916743	HG916721
	CCF 4679 = CMF ISB 2663	Czechia, Ječmeniště, National Nature Monument, soil, 2012, A. Nováková	HG915908	HG916701	HG916744	HG916722
	CCF 4680	Spain, Andalusia, Nerja Cave, cave sediment, 2012, A. Nováková	HG915909	HG916702	HG916745	HG916723
	CCF 4697	Spain, Andalusia, Nerja Cave, cave air, 2012, A. Nováková	HG915910	HG916703	HG916746	HG916724
	EMSL 4874	USA, Georgia, Sandersville, crawlspace (swab), 2018, Ž. Jurjević	**MW448677**	**MW478506**	**MW478525**	**MW478554**
	CCF 4886 = S716	Spain, Andalusia, Nerja Cave, cave sediment, 2012, A. Nováková	LM999908	LM644272	HG916748	LM644259

(*continued on next page*)

Table 1. (Continued).

Species	Strain numbers[1]	Provenance (substrate, locality, year of isolation, collector/isolator)	GenBank/EMBL accession numbers[2]			
			ITS rDNA	*benA*	*CaM*	*RPB2*
	CCF 4829 = BMP 3043	USA, Arizona, Benson, Kartchner Caverns, speleothem surface, 2008, M. Vaughan	HQ832962	LM644273	LM644253	LM644255
	CBS 115952	Germany, dust, S. Ammermann	**MW448678**	**MW478507**	**MW478526**	**MW478555**
	UTHSCSA DI17-89 (UTHSCSA 04-3307)	USA, Missouri, human forearm, 2004, D. Sutton	LT899491	LT899538	LT899593	LT899648
	FMR 14606	Spain, Balearic Islands, Mallorca, soil, 2012, J. Gené	LT899488	LT899537	LT899590	LT899645
	FMR 15176	Spain, Balearic Islands, Mallorca, herbivore dung, 2016, J. Gené & J.P.Z. Siqueira	LT899489	LT798972	LT899591	LT899646
	FMR 15223	Spain, Balearic Islands, Mallorca, herbivore dung, 2016, J. Gené & J.P.Z. Siqueira	LT899490	LT798976	LT899592	LT899647
	CCF 6263 = EMSL 4125	USA, New Jersey, Marlton, black walnut (*Juglans nigra*), 2017, Ž. Jurjević	**MW448679**	**MW478508**	**MW478527**	**MW478556**
	CCF 6248 = EMSL 4140	USA, New Jersey, Marlton, black walnut (*Juglans nigra*), 2017, Ž. Jurjević	**MW448680**	**MW478509**	**MW478528**	**MW478557**
A. suttoniae	UTHSCSA DI14-215^T = FMR 13523^T	USA, human sputum, 2014, D. Sutton	LT899487	LT899536	LT899589	LT899644
A. templicola	CBS 138181^T = DTO 270-C6^T	Mexico, Sayulita, dust from church, 2010, E. Whitfield & K. Mwange	KJ775545	KJ775092	KJ775394	KP987017
	CBS 138180 = DTO 267-H4	Thailand, Bangkok, house dust, 2010, E. Whitfield & K. Mwange	KP987081	KJ775087	KP987064	KP987038
	NRRL 62825 = CCF 4698 = CMF ISB 2662 (ex-type of *A. mangaliensis*)	Romania, Mangalia, soil near Moville Cave, 2012, A. Nováková	HG915902	HG916695	HG916738	HG916716
	CCF 869 = NRRL 62823	China, industrial material, 1955, V. Zánová	HG915903	HG916696	HG916739	HG916717
	NRRL 4893 = IMI 343701 = CCF 4846	Japan, soil	LM999907	LM644271	LM644242	LM644256
	IHEM 14393	Belgium, Charleroi, furniture in hospital 1998, BCCM/IHEM collection	**MW448681**	**LN909024**	**MW478529**	**MW478558**
	DK-T43978	Denmark, Copenhagen, bronchoalveolar lavage, 2014	**MW448682**	**LN909025**	**MW478530**	**MW478559**
A. urmiensis	CBS 139558^T = CCTU 742^T = DTO 203-C2^T = IBT 32593^T	Iran, Urmia, Jade Darya (seaside), soil, 2011, U. Ghosta & R. Samadi	KP987073	KP987041	KP987056	KP987030
	CBS 139557 = CCTU 734 = DTO 203-B3 = IBT 32597	Iran, Jade Darya (seaside), soil, 2011, U. Ghosta & R. Samadi	KP987072	KP987039	KP987055	KP987029
	CBS 139766 = CCTU 743 = DTO 203-C3 = IBT 32598	Iran, Jade Darya (seaside), soil, 2011, U. Ghosta & R. Samadi	KP987074	KP987042	KP987057	KP987031

[1] Acronyms of culture collections in alphabetic order: ATCC, American Type Culture Collection, Manassas, Virginia, USA; BMP, Barry M. Pryor laboratory culture collection, Tucson, Arizona, USA; CBS, Westerdijk Fungal Biodiversity Institute (formerly Centraalbureau voor Schimmelcultures), Utrecht, the Netherlands; CCF, Culture Collection of Fungi, Department of Botany, Charles University, Prague, Czech Republic; CMF ISB, Collection of Microscopic Fungi of the Institute of Soil Biology, Academy of Sciences of the Czech Republic, České Budějovice, Czech Republic; CCTU, Culture Collection of Tabriz University, Tabriz, Iran; FMR, Faculty of Medicine, Reus, Spain; FRR, Food Fungal Culture Collection, North Ride, Australia; IFM, Collection at the Medical Mycology Research Center, Chiba University, Chiba, Japan; IHEM (BCCM/IHEM), Belgian Coordinated Collections of Micro-organisms, Fungi Collection: Human and Animal Health, Sciensano, Brussels, Belgium; IMI, CABI's collection of fungi and bacteria, Egham, UK; NRRL, Agricultural Research Service Culture Collection, Peoria, Illinois, USA; UTHSCSA, Collection of Fungus Testing Laboratory, University of Texas, Health Science Center, San Antonio, USA.

[2] Sequences generated in this study are designated by bold print.

Table 2. Alignment characteristics and substitution models according to Bayesian Information Criterion.[1]

Dataset (Series)	**Locus**	**Alignment length**	**Variable sites**	**Parsimony informative sites**	**Substitution model**
Flavipedes	*benA*	512	138	102	K80+G
	CaM	560	144	116	TrNef+G
	RPB2	1 013	161	129	TrNef+G
	ITS rDNA	539	14	12	F81+I
Spelaei	*benA*	507	127	108	K80+G
	CaM	731	193	164	TrNef+G
	RPB2	1 009	138	113	TrNef+G
	ITS rDNA	549	21	13	HKY

[1] proposed by jModelTest v. 2.1.7 (Posada 2008).

species series and phylogenetically distinct from series *Flavipedes* and *Spelaei*. The ITS rDNA region was excluded due to its low number of informative sites. Omission of the ITS region from the phylogenetic analysis is a common practice as discussed previously (Chen *et al.* 2017). The following steps were performed separately for both datasets.

The *haplotype* function from R v. 4.0.2 (R Core Team 2015) package PEGAS (Paradis 2010) was used to retain only unique sequences in alignments. The best fitting models obtained in jModelTest v. 2.1.7 (Posada 2008) are listed in Table 2.

We used one multi-locus method, STACEY (Jones 2017), and four single-locus species delimitation methods, GMYC (Fujisawa & Barraclough 2013), bGMYC (Reid & Carstens 2012), PTP and bPTP (Zhang *et al.* 2013), to create hypotheses about species boundaries. The multi-locus species delimitation analysis was performed in BEAST v. 2.6.3 (Bouckaert *et al.* 2014) add-on STACEY v. 1.2.5 (Jones 2017) with the following parameters. The chain length was set to 1×10^8 generations, the *species tree* prior was set to the Yule model, *growth rate* prior was set to lognormal distribution (M = 5, S = 2), *clock rate* priors for all loci were set to lognormal distribution (M = 0, S = 1), *PopPriorScale* prior was set to lognormal distribution (M = -7, S = 2) and *relativeDeathRate* prior was set to beta distribution (α = 1, β = 1 000). The output was processed with SpeciesDelimitationAnalyzer (Jones 2017). The ultrametric input trees for the GMYC method (Fujisawa & Barraclough 2013) were calculated in BEAST v. 2.6.3 (Bouckaert *et al.* 2014) with chain length 1×10^7 generations. The GMYC analysis was performed in R v. 4.0.2 (R Core Team 2015) with the package SPLITS (Fujisawa & Barraclough 2013). One hundred ultrametric trees from the BEAST v. 2.6.3 inference were randomly selected using R v. 4.0.2 package APE (Paradis *et al.* 2004) after discarding the initial 25 % of the trees as burn-in, and then used as input for the bGMYC method. The analysis was performed in R v. 3.4.1 with package BGMYC (Reid & Carstens 2012). One thousand maximum likelihood standard bootstrap trees were calculated in IQ-TREE v. 2.0 (Nguyen *et al.* 2015) and used as input for PTP method. The analysis was run in Python v. 3 (van Rossum & Drake 2019) package PTP (Zhang *et al.* 2013). The bPTP was also performed in Python package PTP (Zhang *et al.* 2013). Recommended inputs for this method are trees from Bayesian inference, but without the requirement of ultrametricity. In this case, we used trees from a mcmc run in MrBayes v. 3.2.7 (Ronquist *et al.* 2012). Phylogenetic trees generated during STACEY analysis were used for the presentation of species delimitation results analysis. The graphical outputs were created in iTOL (Interactive Tree Of Life) (Letunic & Bork 2016).

Finally, we tested different species boundaries hypotheses in DELINEATE (Sukumaran et al. 2021). The analysis was performed according to the manual available online. Briefly, the dataset was split into hypothetical populations with "A10" analysis in BPP v. 4.3 (Yang 2015) (Supplementary Table S1). The starBEAST (Heled & Drummond 2010) implemented in BEAST v. 2.6.3 (Bouckaert *et al.* 2014) was used to estimate the species tree. The populations delimited by BPP were lumped into species based on the results of species delimitation methods and phenotypic characters, with several populations always left unassigned to be delimited by DELINEATE. Four models of species boundaries were set up for the *Flavipedes* series, 14 models for the *Spelaei* series and six models for both series analyzed together. The analysis was run in Python v. 3 (van Rossum & Drake 2019) package DELINEATE (available online https://jeetsukumaran.github.io/delineate/).

Phenotypic studies

The macromorphology of colonies was studied on Czapek yeast autolysate agar (CYA; Fluka, Buchs, Switzerland), Czapek-Dox agar (CZA), malt extract agar (MEA; Oxoid, Melbourne, Australia) (Samson *et al.* 2014), oatmeal agar (OA; Difco, La Ponte de Claix, France) and CYA supplemented with 20 % sucrose (CY20S). The strains were inoculated in three points on 90 mm Petri dishes and incubated at 25 °C in darkness. Cardinal temperatures were determined for *A. movilensis* and its relatives. The strains were grown on MEA for 14 d at 10, 15, 20, 25, 30, 35, 37 and 40 °C in darkness. For the description of colony colours, we used the hexadecimal colour codes and the names were assigned according to website https://coolors.co/. Colony details were documented using an Olympus SZX2-ILLT dissecting microscope (Tokyo, Japan) equipped with an Olympus DP27 digital camera.

Micromorphological characters were observed from 14-d-old colonies grown on MEA. Every character was measured 35 times for each isolate. Lactic acid (60 %) was used as the mounting medium. Photographs were taken using an Olympus BX51 microscope with an Olympus DP72 camera. The picture processing and preparation of photographic plates was done in Adobe Photoshop CS6.

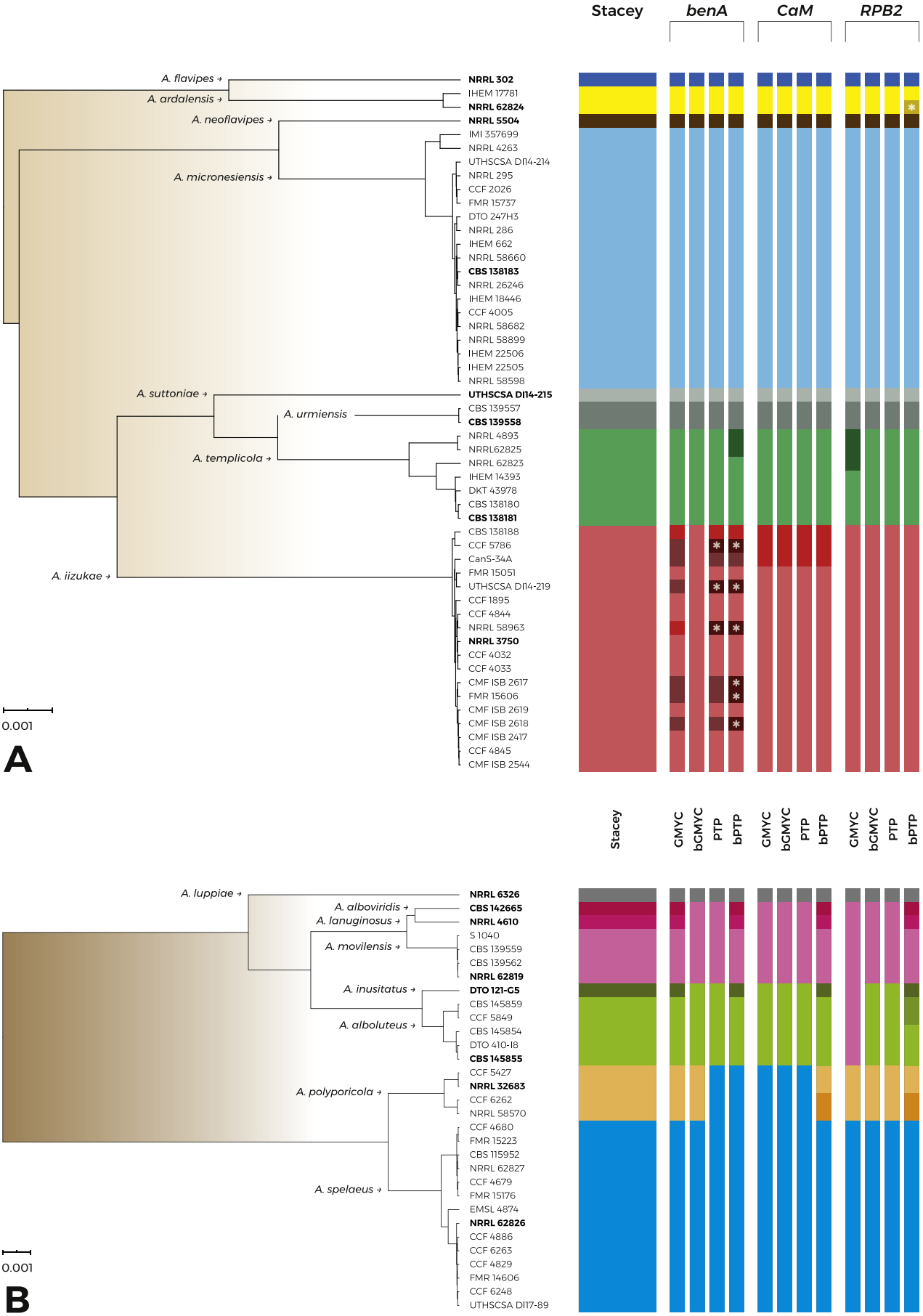

Fig. 1. Schematic representation of species delimitation results in the series *Flavipedes* (A) and *Spelaei* (B). The analyses were based on three loci (*benA*, *CaM*, *RPB2*) and utilized one multi-locus method (STACEY) and four single-locus methods (GMYC, bGMYC, PTP, bPTP). Only strains with unique haplotypes were used (strains with identical sequences are represented by one tip in the tree). The results are depicted by coloured bars with different colours indicating tentative species delimited by each method. The asterisk (*) sign designates singleton species delimited by the particular methods. Ex-type isolates are highlighted with bold font. The phylogenetic tree was calculated during STACEY analysis and is used solely for the comprehensive presentation of the results from different methods.

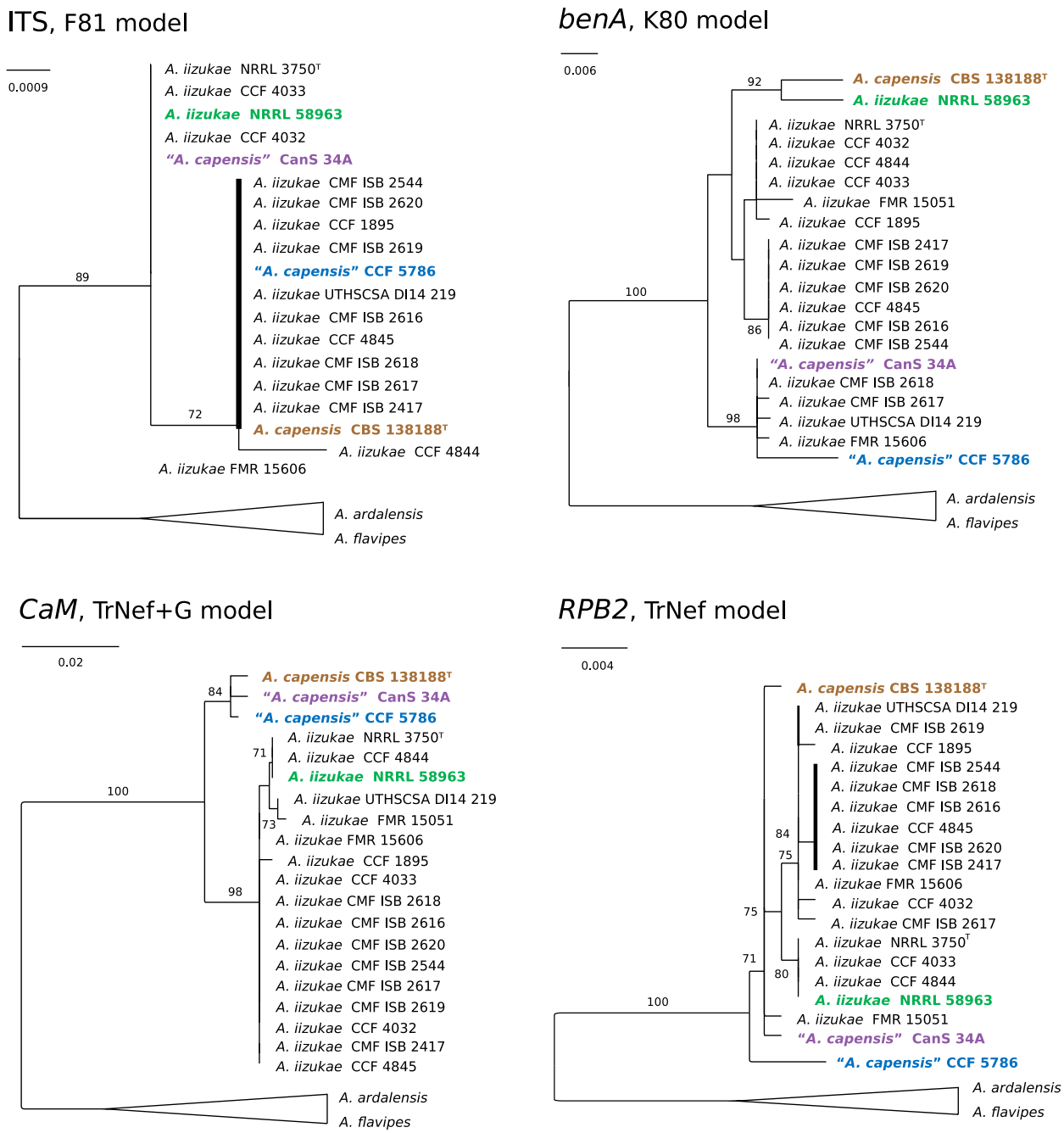

Fig. 2. Single-locus Maximum Likelihood trees of clade containing isolates of *Aspergillus iizuake* and "*A. capensis*". The trees were calculated in IQ-TREE v. 2.0 based on sequences of ITS region and *benA*, *CaM* and *RPB2* loci. The ex-type isolates are designated by a superscript T. The strains with unstable position across phylogenies and thus causing incongruences are highlighted by colours.

Antifungal susceptibility testing (EUCAST method)

The determination of the minimum inhibitory concentrations (MICs) of antifungal agents was carried out according to the reference European Committee on Antimicrobial Susceptibility testing (EUCAST) guidelines (E.Def 9.3.2). Pure antifungal substances were stored in aliquots at -80 °C and stock solutions prepared in DMSO (5 000 mg/L; Sigma-Aldrich, Brøndby, Denmark). Cell-culture-treated NuncTM MicroWellTM 96-Well Microplates (ThermoFisher Scientific, catalogue no. 167008) were used throughout. Microtitre plates with 2-fold dilutions were prepared using serial dilution (with two pipette tip changes) and frozen at -80 °C for at least 24 h prior to use. The following antifungal agents (final concentration ranges) were included: amphotericin B (0.004–4 mg/L; Sigma-Aldrich, Germany), itraconazole (0.004–4 mg/L and 0.016–16 mg/L; Sigma-Aldrich), posaconazole (0.004–4 mg/L; MSD, Ballerup, Denmark), voriconazole (0.004–4 mg/L and 0.016–16 mg/L; Pfizer A/S, Ballerup, Denmark and Sigma-Aldrich), isavuconazole (0.008–8 mg/L and 0.016–16 mg/L; Basilea Pharmaceutica International Ltd, Basel, Switzerland), and terbinafine (0.004–4 mg/L; Sigma-Aldrich). Two concentration ranges for some antifungals were used because the isolates were analyzed in two batches and, as the breakpoints are low, we decided to skip the highest concentrations for the second batch and move the range toward lower concentrations. Plates were incubated at 37 °C (or 25 °C for species with insufficient growth at 37 °C) for 48 h. *Aspergillus fumigatus* ATCC 204305 was included as quality control (Arendrup *et al.* 2021).

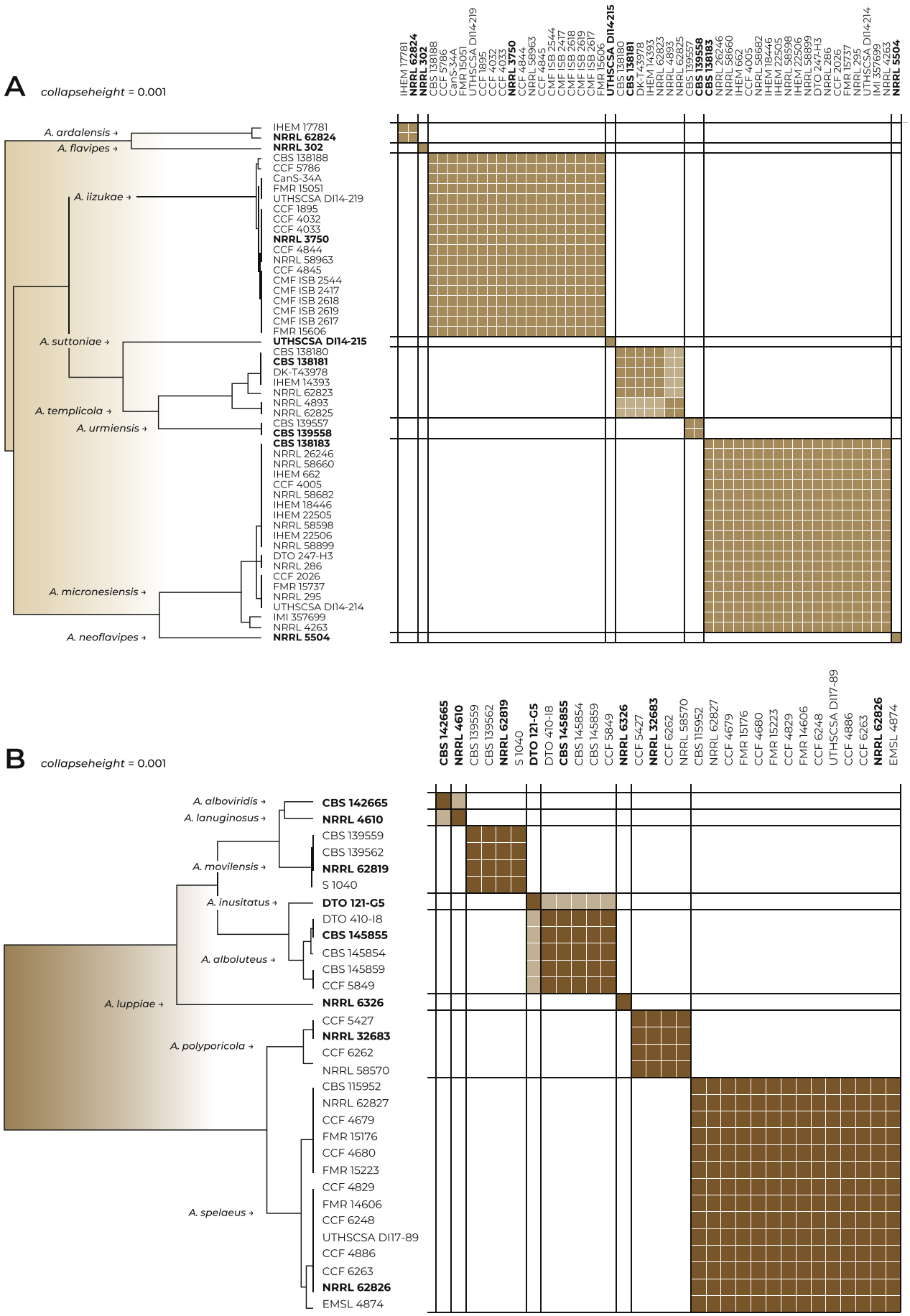

Fig. 3. The results of species delimitation by STACEY add-on of BEAST v. 2 in the series *Flavipedes* (A) and *Spelaei* (B) with the chosen *collapseheight* parameter = 0.001. The similarity matrices give the posterior probability of every two isolates belonging to the same multi-species coalescent cluster (tentative species). The darkest brown shade corresponds to a posterior probability of 1, while a white colour is equal to 0. The horizontal and vertical lines in the similarity matrices depict the species boundaries proposed by the analysis. Only strains with unique multilocus haplotypes were used in the analysis (strains with identical haplotype are represented by one tip in the tree). Ex-type isolates are highlighted with bold font. Presented phylogenetic trees were calculated in STACEY.

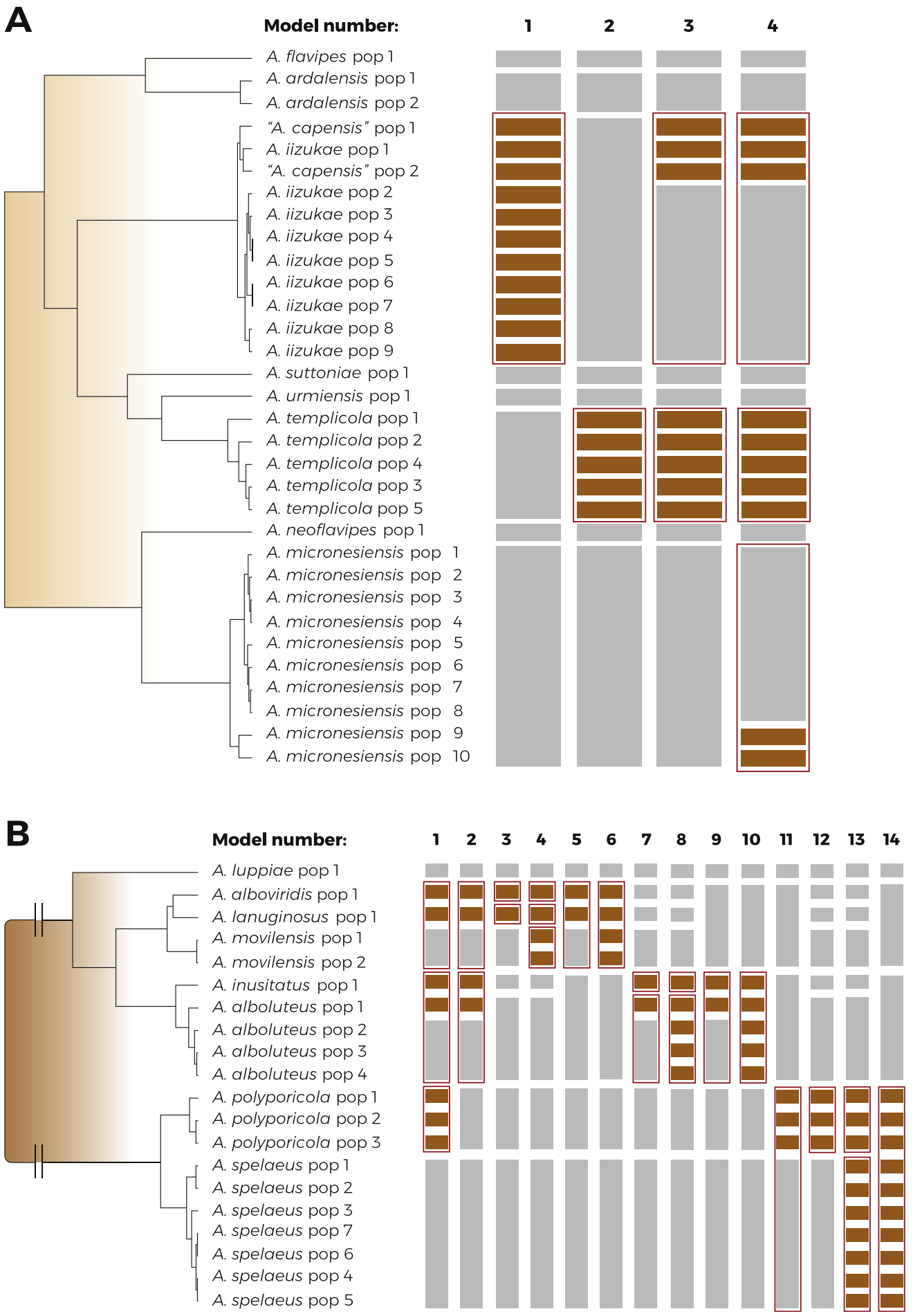

Fig. 4. The results of species validation using DELINEATE in the series *Flavipedes* (A) and *Spelaei* (B). The populations of each species were delimited by BPP (Supplementary Table S1) and the displayed tree was calculated in starBEAST. The bars on the right side of the tree depicts the setting and results of each model. The grey bars represent the predefined species (locked in the analysis), while the brown bars represent unassigned populations left free to be delimited. The red rectangles depict the resulting solution proposed by DELINEATE.

RESULTS

The species delimitation analyses were mostly divided into two parts corresponding to the series *Flavipedes* and *Spelaei* according to Houbraken *et al.* (2020). The analysis of each series consisted of two steps (for detailed description see Materials and Methods).

Species delimitation and validation in the series *Flavipedes*

The results of various species delimitation methods in the series *Flavipedes* (Fig. 1A) were in broad agreement and unequivocally supported the species *A. flavipes*, *A. neoflavipes*, *A. micronesiensis*, *A. suttoniae* and *A. urmiensis*. *Aspergillus ardalensis* was split into two tentative species by bPTP using *RPB2* as input, but a broader concept was supported by all other methods (Fig. 1A). Similarly, *A. templicola* was split into two tentative species by GMYC using *RPB2* as input and by bPTP using *benA* as input; but all other methods resolved *A. templicola* as a single species. Less stable results were obtained in the node comprising *A. iizukae* and *A. capensis*. All single-locus methods delimited "*A. capensis* lineage" represented by CBS 138188^{T}, CCF 5786 and CanS-34A as separate species using *CaM* as input. When *benA* was used as input, the methods showed variable results. The bGMYC method lumped *A. capensis* and *A. iizukae* together, PTP and bPTP delimited several singleton species and GMYC delimited three species (with *A. capensis* consisting of CBS 138188^{T} and *A. iizukae* strain NRRL 58963). These results together with unstable position of particular strains in single-locus trees (Fig. 2) suggest ongoing recombination within the clade formed by *A. iizukae* and *A. capensis*.

Detailed results of STACEY (Fig. 3A and Supplementary Fig. S1 with different values of *collapseheight* parameter) with similarity matrix displaying the probability of assignment of strains to particular species suggest that the support for splitting *A. iizukae*/*A. capensis* into two species is lower than in other species, *e.g.*, in *A. templicola* or *A. micronesiensis* which were not split by any single-locus species delimitation methods.

In the species validation step (Fig. 4A), we set up four different models focusing mainly on *A. iizukae*/*A. capensis* clade. The first model left all populations of *A. iizukae* and *A. capensis* delimited by BPP (Yang 2015) (Supplementary Table S1) unassigned into species, *i.e.*, free to be delimited. These unassigned populations are depicted by brown coloured bars in the Fig. 4, while populations of other species were assigned according to the delimitation in the first step - grey bars. As a result, *A. iizukae* and *A. capensis* populations were lumped together into one species - depicted by red rectangle around bars (Fig. 4A). In the second model, populations of *A. templicola* were left unassigned and the results lumped them together within one species. Third and fourth model left unassigned all populations of *A. templicola* and several populations of "*A. capensis*", *A. iizukae* and *A. micronesiensis* and the results always supported broad species definition of *A. templicola*, *A. miconesiensis* and *A. iizukae* (comprising *A. capensis*). Overall, the results supported all currently accepted species within series *Flavipedes* with the exception of *A. capensis*, which is therefore placed in synonymy with *A. iizukae*. This finding is also supported by morphological observations as *A. iizukae* and *A. capensis* are not distinguishable (Visagie *et al.* 2014).

Species delimitation and validation in the series *Spelaei*

The species delimitation in the series *Spelaei* was less clear compared to series *Flavipedes*. Based on the results described below, we decided to introduce four new species, namely *Aspergillus alboluteus*, *A. alboviridis*, *A. inusitatus* and *A. lanuginosus* (see section Taxonomy).

In the first part of the analysis *A. luppiae* was the only species delimited by all methods without any exception (Fig. 1B). *Aspergillus spelaeus* and *A. polyporicola* were lumped together by PTP and bPTP using *benA* as input, and also by GMYC, bGMYC and PTP using *CaM* as an input. On the other hand, *A. polyporicola* was split into two species by bPTP using *CaM* and *RPB2* as input. The four newly described species *A. alboluteus*, *A. alboviridis*, *A. inusitatus* and *A. lanuginosus* were all delimited by GMYC using *benA* and bPTP using all three genes (*A. alboluteus* was even divided into two species by bPTP using *RPB2* as an input). The GMYC method with *RPB2* as input delimited only one species in this clade, containing the four mentioned species and *A. movilensis*; and the remaining methods based on *RPB2* delimited two species. If only these results would be considered, it might not be enough to support delimitation of five species, but there were striking morphological differences (see section Phenotype analysis) supporting the narrower species concept. This is also in agreement with the results of a multi-locus method STACEY which supported all five species in this clade, and at the same time supported the recognition of *A. spelaeus* and *A. polyporicola* as separate species (Fig. 1B). Especially the morphology of *A. inusitatus* does not allow its inclusion into any other species and denies the possibility of a broader concept in this clade.

Detailed results of STACEY show that when the *collapseheight* parameter is low enough to consider *A. inusitatus* a separate species (Fig. 3B and Supplementary Fig. S2B), the clade containing *A. movilensis* should be also split into three species (*A. movilensis*, *A. alboviridis* and *A. lanuginosus*). If the *collapseheight* parameter is too high (Supplementary Fig. S2A) to delimit *A. inusitatus*, also the support for *A. polyporicola* and *A. spelaeus* decreases.

In the species validation step (Fig. 4B), we set up 14 different models for testing the species hypotheses. The first model left unassigned populations of *A. alboviridis*, *A. lanuginosus*, *A. inusitatus*, *A. polyporicola* and population 1 of *A. alboluteus*. The results supported *A. polyporicola* but lumped together *A. inusitatus*/*A. alboluteus* and *A. movilensis*/*A. alboviridis*/*A. lanuginosus*. The results of the second model with similar setting except for predefined species status of *A. polyporicola* were identical. In the third and fourth model, *A. inusitatus* and *A. alboluteus* were defined as separate species. *Aspergillus alboviridis* and *A. lanuginosus* were left unassigned in the third model and in the fourth model, *A. alboviridis*, *A. lanuginosus* and *A. movilensis* were left unassigned. The results were similar in both cases, recognizing *A. alboviridis*, *A. lanuginosus* and *A. movilensis* as separate species. The fifth and sixth model were analogous to model 3 and 4, leaving *A. alboviridis* and *A. lanuginosus* (model 5); and *A. alboviridis*, *A. lanuginosus* and

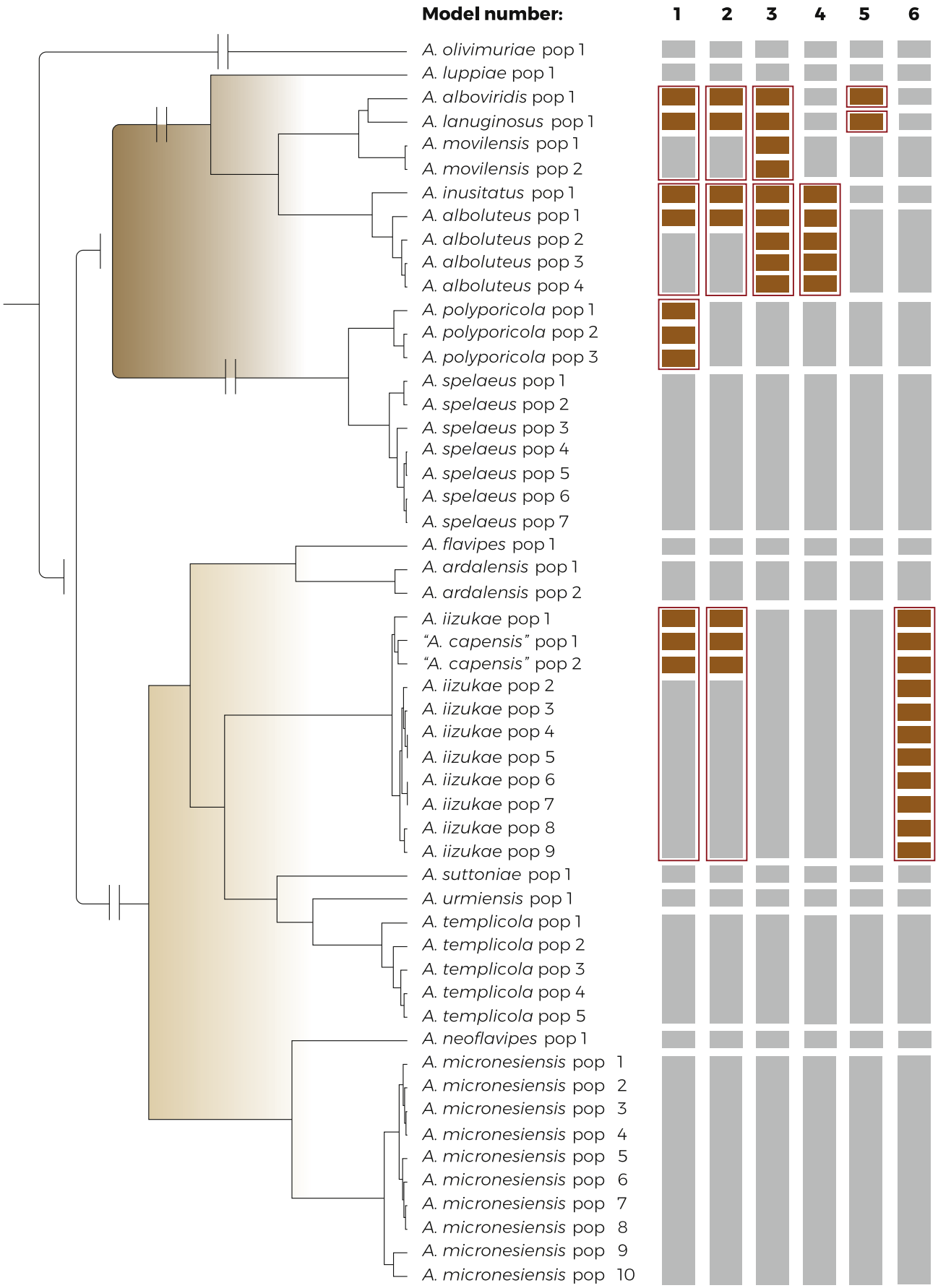

Fig. 5. The results of species validation using DELINEATE for the series *Flavipedes* and *Spelaei* analyzed together. The populations of each species were delimited by BPP (Supplementary Table S1) and the displayed tree was calculated in starBEAST. The bars on the right side of the tree depicts the setting and results of each model. The grey bars represent the predefined species (locked in the analysis), while the brown bars represent unassigned populations left free to be delimited. The red rectangles depict the resulting solution proposed by DELINEATE.

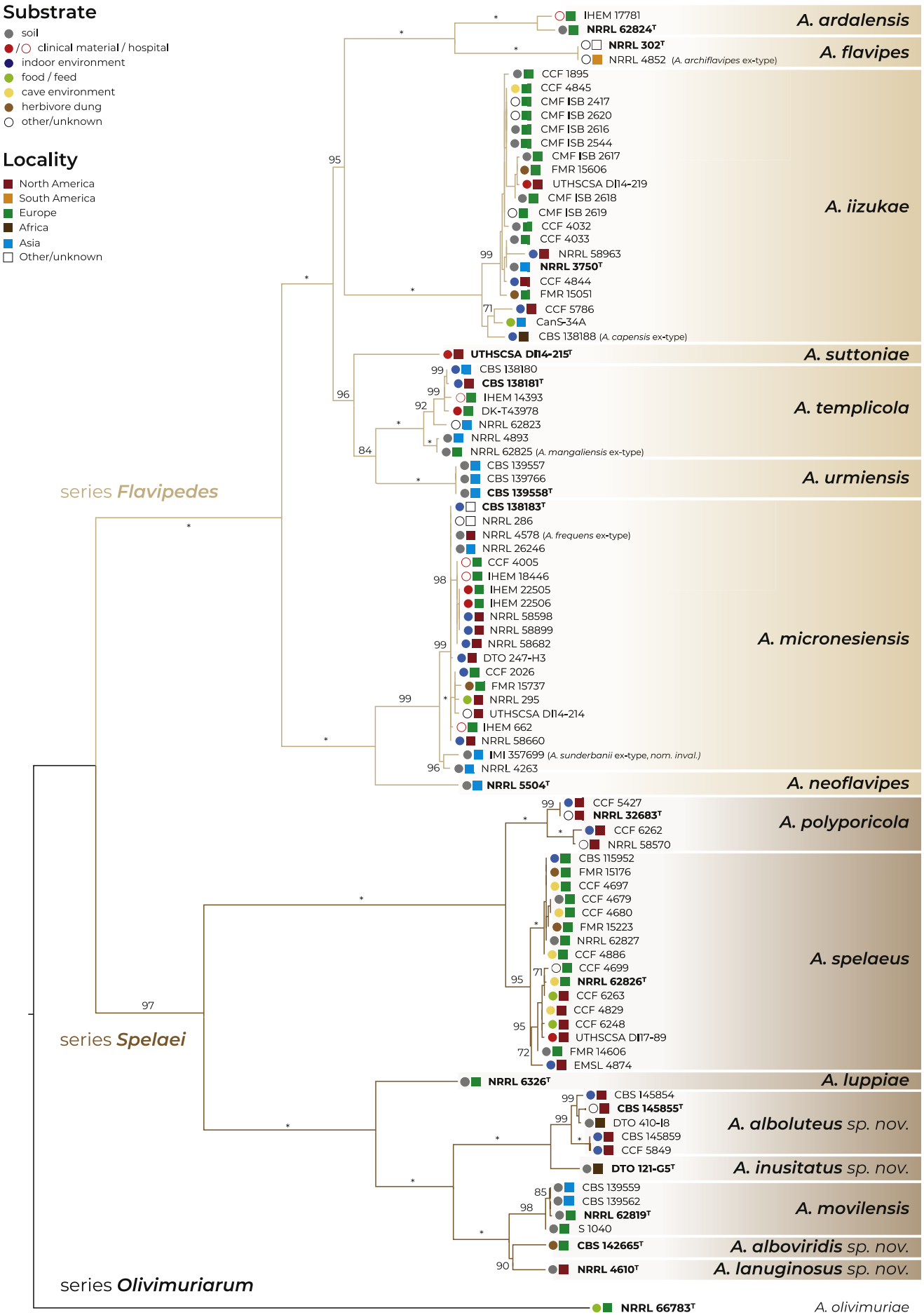

Fig. 6. Phylogenetic relationships of the section *Flavipedes* members inferred by Maximum Likelihood analysis in IQ-TREE v. 2.0 using concatenated alignment of four loci ITS, (*benA*, *CaM*, *RPB2*). The bootstrap support values are appended to nodes (only those supported by bootstrap value of 70 % or higher are displayed) with asterisks indicating the full support. Ex-type isolates are designated by bold font and superscript T. The names of species treated as synonyms are listed in parentheses. The source and locality of isolation are indicated by coloured circles and squares, respectively.

Table 3. Overview of selected phenotypic characters for section *Flavipedes* members.[1]

Species	Growth parameters after 7 days					Prevailing colony colours on CYA and MEA	Conidia: diam (µm)[4], surface	Vesicle diam (µm)	Stipe (µm)		Hülle cells[2]	Sex. state
	CYA	CZA	MEA	37 °C	40 °C				Length	Width		
A. alboluteus	15–27	10–20	13–26	+	—	white, yellow	2.5–3.5, smooth	(6–)9–17(–20)	(500–)800–1200(–2000)	4–7(–10)	+	—
A. alboviridis	19–21	9–10	18–23	+[3]	—	light green, white, yellow	2.5–3.5, smooth	12–16(–20)	120–200(–550)	4.5–6(–8)	+	—
A. ardalensis	25–28	20–28	25–28	+	+	pale ochreous, yellow	2.5–3, smooth	(5–)7–19	commonly >1000	3–8(–9)	+	—
A. flavipes	25–35	25–28	25–35	+	—	white, yellowish-white, pale ochreous	2–3, smooth	7–11	occasionally >1000	3–6	—	—
A. iizukae	16–35	13–25	13–30	+	—	yellowish-white, yellow, ochreous, brown, greyish-brown	2–3(–3.5), smooth	(6–)14–20(–35)	200–1500	(3.5–)5–10(–13.5)	+	—
A. inusitatus	22–23	8–9	17–19	+	+[3]	dark green, yellow	3.5–4, echinulate	15–18	250–600	5–6	+	—
A. lanuginosus	26–27	21–22	20–21	+	—	white, light pinkish-brown, pale ochreous	2.5–3, smooth	10–12	600–1100	3.5–4.5	—	—
A. luppiae	18–20	17–21	20–22	+	—	yellow, white	2.5–3.5, smooth	11–16	100–220(–300)	3.5–5.5	+	—
A. micronesiensis	14–30	9–25	18–28	+	—	yellowish-white, yellow, pale ochreous, brown, grayish-brown	(2–)2.5–3.5(–4), smooth	(4–)6–16(–31)	250–1900	2–10	+	—
A. movilensis	22–25	19–20	25–30	+	—	white, pale ochreous, light yellow-green	2.5–3.3(–3.5), smooth	(5–)9–13(–16)	usually <400, occasionally >1000	3.5–6	+	—
A. neoflavipes	17–21	18–20	18–22	+	+[3]	yellow, white	(2–)2.5–3, smooth	13–19	250–950	5–7.5	+	+
A. neoniveus	15–16	12–14	13	—	—	yellow, white	2–2.5, smooth	9–11	150–300	4.5–6	+	+
A. olivimuriae	31–35	23–28	24–27	+	—	ochreous	2–2.5, smooth	8–10(–15)	100–150	5–6	—	—
A. polyporicola	17–27	14–20	20–32	—	—	pale ochreous, ochreous	2–3(–3.5), smooth	(6–)8–16(–20)	250–1000	3.5–6(–9)	—	—
A. spelaeus	16–30	6–26	15–32	—	—	pale ochreous, ochreous	2–3(–3.5), smooth	(5–)7–18(–23)	400–1000, occasionally >1000	3–7(–9)	+	—
A. suttoniae	24–25	20–22	24-25	+	—	yellowish-white, ochreous	2–3.5, smooth	(6–)12–17	180–420	4.5–6.5	—	—
A. templicola	21–32	21–28	23–30	+	+[3]	white, yellowish-white, pale ochreous	2–3, smooth	(6–)9–23	120–1400	3.5–10	+	—
A. urmiensis	28–32	20–24	23–27	+	—	white, ochreous	2–3, smooth	(17–)20–23(–30)	(350–)700–850(–1330)	(5–)8–10(–12)	—	—

"—" indicate no growth or absence of character/structure in culture.

[1] Based on data from this study, Visagie *et al.* (2014), Hubka *et al.* (2015), Arzanlou *et al.* (2016), Siqueira *et al.* (2018), Crognale *et al.* (2019).

[2] Production may vary between isolates and depend on cultivation conditions.

[3] Very restricted growth ($\leq$ 2 mm).

[4] Conidia of all species are globose or subglobose, and only the longer dimension is given in case of subglobose conidia.

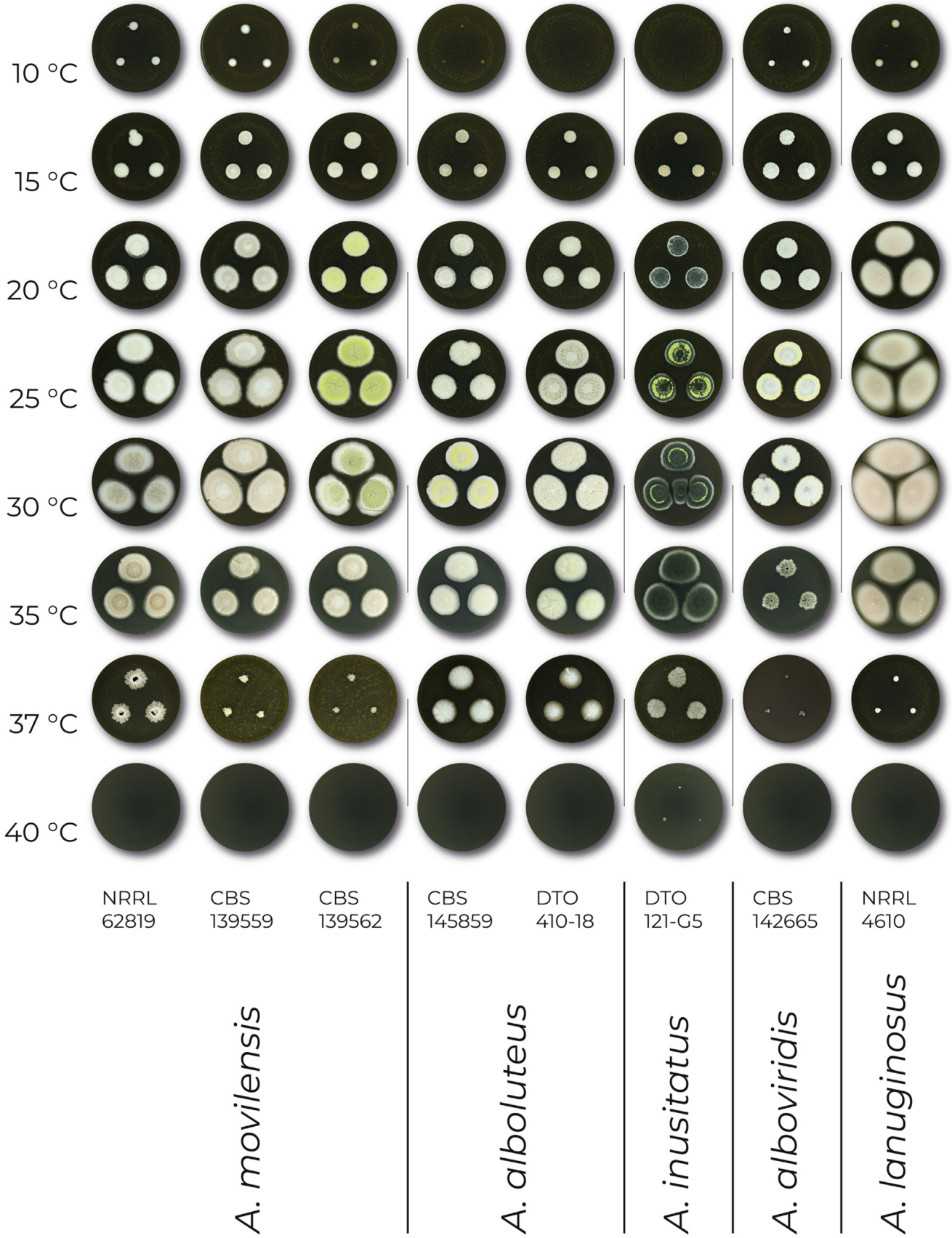

Fig. 7. Temperature growth profile in the newly described species and *Aspergillus movilensis* after 14 d on MEA at temperatures ranging from 10 °C to 40 °C.

A. movilensis (model 6), respectively, free to be delimited. Unlike models 3 and 4, in case of models 5 and 6, *A. inusitatus* was predefined as a part of *A. alboluteus*. These models resulted in lumping of *A. alboviridis, A. lanuginosus* and *A. movilensis* into one species. The models 7–10 tested the opposite hypothesis, leaving *A. inusitatus* and either one population (models 7 and 9) or all populations (models 8 and 10) of *A. alboluteus* unassigned, and *A. alboviridis* and *A. lanuginosus* predefined either as separate species (models 7 and 8) or lumped together with *A. movilensis* (model 9 and 10). The final results corresponded

with models 3–6. In case of *A. alboviridis*, *A. lanuginosus* and *A. movilensis* being defined as separate species, *A. inusitatus* and *A. alboluteus* were also delimited as separate species (models 7 and 8). If *A. alboviridis*, *A. lanuginosus* and *A. movilensis* were lumped together, *A. inusitatus* and *A. alboluteus* were also lumped into one species (models 9 and 10). Models 11–14 focused on *A. polyporicola* and *A. spelaeus*. Models 11–12 left all populations of *A. polyporicola* free to be delimited and models 13–14 left all populations of both *A. polyporicola* and *A. spelaeus* unassigned. Models 11 and 14 defined *A. alboviridis* and *A. lanuginosus* as a part of *A. movilensis* and *A. inusitatus* as a part of *A. alboluteus*. This resulted in lumping of *A. polyporicola* and *A. spelaeus* into one species. In models 12–13, *A. alboviridis*, *A. lanuginosus*, *A. movilensis*, *A. inusitatus* and *A. alboluteus* were all defined as separate species. This definition resulted in delimitation of *A. polyporicola* and *A. spelaeus* as two separate species.

Species validation in the section *Flavipedes*

Finally, we further validated the putative species in DELINEATE based on the combined dataset of both series using six different models (Fig. 5). The first model left unassigned *A. alboviridis*, *A. lanuginosus*, *A. inusitatus*, population 1 of *A. alboluteus*, *A. polyporicola* and "*A. capensis*" (strains CBS 138188, CanS 34A, and CCF 5786). The second model used the same assignment except for *A. polyporicola*. The results of both models lumped *A. capensis* together with *A. iizukae*; *A. polyporicola* was delimited as separate species; *A. inusitatus* was lumped with *A. alboluteus*; and *A. alboviridis* and *A. lanuginosus* were lumped with *A. movilensis*. The third model left unassigned *A. alboviridis*, *A. lanuginosus*, *A. inusitatus* and also all populations of *A. movilensis* and *A. alboluteus*. The results lumped together *A. alboviridis*/*A. lanuginosus*/*A. movilensis* and *A. inusitatus*/*A. alboluteus*. The fourth model left unassigned *A. inusitatus* and populations of *A. alboluteus* with *A. alboviridis*, *A. lanuginosus* and *A. movilensis* being defined as three separate species and it resulted in *A. inusitatus*/*A. alboluteus* lumped together. On the contrary, the fifth model left *A. alboviridis* and *A. lanuginosus* unassigned with *A. inusitatus*, *A. alboluteus* and *A. movilensis* predefined as separate species, and it resulted in delimitation of separate *A. alboviridis* and *A. lanuginosus*. The sixth model predefined separately all mentioned species except for populations of "*A. capensis*" and *A. iizukae* which were left free to be delimited. This model again resulted in lumping of these two species.

Phylogeny

The Fig. 6 shows the best scoring Maximum likelihood (ML) tree based on the concatenated alignment of 90 strains from section *Flavipedes* representing known species diversity. All deep nodes gained bootstrap support of at least 95 % except for the lineage containing *A. templicola* and *A. urmiensis*. This node with support of 84 % is also the only site of incongruence between the concatenated tree and the tree generated by starBEAST during DELINEATE analysis. In the starBEAST analysis, *A. iizukae* formed a clade with *A. suttoniae*, *A. templicola*, and *A. urmiensis* (Fig. 5), while in the ML tree, *A. iizukae* was sister to the clade containing *A. flavipes* and *A. ardalensis*. Otherwise the topology of these two trees was identical. The only other node with lower support was the lineage comprising two singleton species, *A. alboviridis* and *A. lanuginosus*, with the bootstrap support of 90 %.

Apart from *A. capensis* (ex-type strain CBS 138188), which is discussed above, several other species names are treated here as synonyms in agreement with previous studies. The ex-type strain of *A. archiflavipes* NRRL 4852 is a synonym of *A. flavipes*; *A. mangaliensis* with the ex-type strain NRRL 62825 is a synonym of *A. templicola*; *A. frequens* with the ex-type strain NRRL 4578 is a synonym of *A. micronesiensis*; and finally, an invalid name *A. sunderbanii* based on the strain IMI 357699 is also included in the lineage of *A. micronesiensis* (Fig. 6).

Table 4. Antifungal susceptibility profiles of *Aspergillus* section *Flavipedes* members determined with EUCAST E.Def.9.3 method at 37 °C.[1]

Species (number of tested isolates)	Minimum inhibitory concentration (mg L^{-1})											
	Amphotericin B		Itraconazole		Posaconazole		Voriconazole		Isavuconazole		Terbinafine	
	Range	GM[2]	Range	GM	Range	GM	Range	GM	Range	GM	Range	GM
A. alboluteus (5)	0.125–1	0.44	0.125	0.125	0.06–0.125	0.09	0.25–0.5	0.44	0.5–1	0.76	0.25–0.5	0.33
A. alboviridis (1)	0.5	–	0.25	–	0.125	–	1	–	1	–	4	–
A. ardalensis (2)	1–2	–	0.5–1	–	0.125–1	–	2–8	–	8	–	0.25–1	–
A. flavipes (2)	0.5–2	–	0.06–0.125	–	0.06–0.125	–	0.5–1	–	0.5–1	–	0.125	–
A. iizukae (10)	0.25–2	0.71	0.03–0.25	0.14	0.03–0.25	0.12	0.5–1	0.81	1–8	4	0.25–0.5	0.27
A. inusitatus (1)	1	–	0.06	–	0.03	–	0.25	–	0.5	–	0.125	–
A. lanuginosus (1)	0.125	–	0.03	–	0.03	–	0.125	–	0.25	–	0.25	–
A. luppiae (1)	0.06	–	0.06	–	0.06	–	0.25	–	0.5	–	0.25	–
A. micronesiensis (16)	0.125–1	0.59	0.125–0.5	0.26	0.125–0.5	0.21	0.25–1	0.52	0.5–4	1.24	0.125–0.25	0.23
A. movilensis (4)	0.125–0.25	–	0.03–0.125	–	0.03	–	0.5–1	–	1–2	–	0.125–0.25	–
A. neoflavipes (1)	0.5	–	0.06	–	0.06	–	0.25	–	0.5	–	0.5	–
A. olivimuriae (1)	0.5	–	0.06	–	0.06	–	0.5	–	0.5	–	0.06	–
A. polyporicola (4)[3]	0.25–1	–	0.5	–	0.25–0.5	–	1–2	–	1–2	–	0.25–0.5	–
A. spelaeus (9)[3]	0.5–2	0.79	0.25–1	0.5	0.25–0.5	0.34	1–2	1.47	1–2	1.59	0.25–0.5	0.37
A. suttoniae (1)	0.5	–	0.06	–	0.06	–	0.5	–	1	–	0.25	–
A. templicola (6)	0.125–1	0.4	0.06–0.5	0.22	0.03–0.25	0.11	0.125–0.25	0.22	0.5–1	0.89	0.125–0.25	0.20
A. urmiensis (2)	2–4	–	0.125–0.25	–	0.125–0.25	–	0.25	–	1	–	0.25	–
All isolates (67)	0.06–4	0.57	0.03–1	0.2	0.03–1	0.14	0.125–8	0.62	0.25–8	1.36	0.06–4	0.27

[1]More detailed data are shown in the Supplementary Table S2. Green shading highlights species that are highly susceptible to all the included mould active agents, whereas yellow highlights species for which the MICs to one or more agents are elevated compared to *A. fumigatus* wild-type.

[2]GM, geometric mean - calculated only when ≥5 isolates were tested per species.

[3]MIC determinations performed with 25 °C incubation due to absence of growth at 37 °C.

Before the phylogenetic analysis itself, we tested the phylogenetic position of two relatively distant species, *A. olivimuriae* and *A. neoniveus*. *Aspergillus olivimuriae* was conclusively placed into the section *Flavipedes*, and therefore we included it as an outgroup in the phylogenetic analysis, but it was excluded from the species delimitation analyses. On the other hand, the position of *A. neoniveus* within the section *Flavipedes* did not gain sufficient support and its classification within *Aspergillus* sections remains uncertain. These findings are in agreement with Houbraken *et al.* (2020), who proposed series *Olivimuriarum* (containing only *A. olivimuriae*) and series *Neonivei* (containing only *A. neoniveus*), both within sections *Flavipedes*. In the phylogeny based on the three-gene dataset, the series *Neonivei* made the section *Flavipedes* paraphyletic with respect to section *Terrei*, while in the phylogeny based on nine genes, *A. neoniveus* was resolved within section *Flavipedes* (Houbraken *et al.* 2020).

Phenotype analysis in relatives of *A. movilensis*

Selected culture and micromorphological characteristics relevant for species identification in section *Flavipedes* are summarized in Table 3. In the following paragraphs, we mostly focus on species related to *A. movilensis* because there was no clear consensus on species boundaries across molecular species delimitation methods used in this study.

The colony colours of species from section *Flavipedes* are usually yellow, white, or in shades of brown. Two species newly described in this study are different in this regard. The colour of *A. alboviridis* colonies on some media is light green and *A. inusitatus* produces dark green colonies with yellow clumps of Hülle cells on all tested media. *Aspergillus inusitatus* is the only species with echinulate conidia in the whole section *Flavipedes*. In the study of Hubka *et al.* (2015), the production of accessory conidia has been observed in all section *Flavipedes* species. We expected to find them also in the newly described species, but they were only rarely present in some *A. alboluteus* strains and not observed in the other species. The sexual state has been only observed in *A. neoflavipes* and *A. neoniveus*, and it is produced in a homothallic manner. All other species from the section including all newly described species are presumably heterothallic and do not produce the sexual morph in culture under conditions used in this study.

To support species hypotheses and proposal of new taxa related to *A. movilensis*, we determined cardinal temperatures, compared the macromorphology on five media and the micromorphology of particular strains. Cardinal temperatures were determined on MEA after 14 d of cultivation in darkness at eight different temperatures ranging from 10 °C to 40 °C. The resulting colonies are compared in Fig. 7, which demonstrates phylogenetic pattern in growth rates and abilities to grow at different temperatures. *Aspergillus lanuginosus* grows faster than any other species at 20, 25 and 30 °C. *Aspergillus alboluteus* and *A. insitatus* grow faster at 37 °C than the other three species and unlike the other three species they do not grow at 10 °C (or grow very restrictedly - isolate CCF 6201). *Aspergillus inusitatus* is the only species capable of growing at 40 °C. The colony texture of *A. lanuginosus* is cottony or downy on the majority of media due to the production of abundant aerial mycelium, while the colonies of the other species are rather floccose.

We observed morphological variation between the examined *A. movilensis* strains (Fig. 7). In general, white or grey colonies are produced, but the colonies of CBS 139562 are light green to yellow. We observed that colonies of some species change colour at suboptimal temperatures because of decreased sporulation (Fig. 7). There are differences between species in the ability to produce Hülle cells, which we observed in *A. alboluteus*, *A. alboviridis*, *A. inusitatus*, and *A. movilensis*, but they were not produced by *A. lanuginosus*. The length of stipes can be considered taxonomically important and may be used to distinguish *A. alboviridis* (mostly < 200 µm), *A. movilensis* (mostly < 400 µm), and *A. lanuginosus* (usually 600–1100 µm). Otherwise, the micromorphological characters were rather overlapping between the above-mentioned species.

Ecology

Based on the number of strains included in this study, *A. micronesiensis*, *A. iizukae*, *A. spelaeus* and *A. templicola* seem to be the most commonly encountered species. This is also in agreement with number of *benA* and *CaM* sequences deposited in GenBank for these species. In contrast to ITS region, the *benA* and *CaM* records for these species can be easily identified thanks to barcoding gap visible during BLAST analysis. The recorded numbers for *benA* /*CaM* loci in GenBank are as follows (accessed on June 10 2021) : *A. micronesiensis* 37 / 41, *A. iizukae* 24 / 23, *A. spelaeus* 18 / 18, and *A. templicola* 18 / 11.

The most common and diverse habitat for section *Flavipedes* members is undoubtedly the soil where 12 out of 17 species in our set of strains (excluding *A. neoniveus*) were found (Fig. 6). Our dataset contained five strains isolated from the hospital environment and six strains originating from clinical material. Only one of these strains belonged to the series *Spelaei*, specifically to *A. spelaeus*. The remaining strains were spread throughout the series *Flavipedes*, belonging to *A. iizukae*, *A. suttoniae*, *A. templicola* and *A. micronesiensis*. A significant number of species from both series originated from the indoor environment, namely *A. iizukae*, *A. templicola*, *A. micronesiensis*, *A. polyporicola*, *A. spelaeus* and *A. alboluteus*. In total three species, *A. iizukae*, *A. spelaeus* and *A. alboviridis*, were isolated from herbivore dung. Strains from food and feed were poorly represented in our dataset and restricted to *A. iizukae*, *A. micronesiensis* and *A. spelaeus*. None of the species which were represented by a high number of strains seem to be substrate specific.

Antifungal susceptibility testing (EUCAST method)

The minimum inhibitory concentration (MIC) ranges and geometric mean (GM) values obtained by the EUCAST reference method for six antifungal agents are shown in Table 4 and more detailed results in Supplementary Table S2. Clinical breakpoints have been established for amphotericin B and the mould active azoles against *A. fumigatus*, which is the most common *Aspergillus* species in human infections. Clinical breakpoints have not been established for the *Aspergillus* section *Flavipedes* members. A general rule of thumb is that species that rarely cause disease in humans are less pathogenic, and therefore that adopting the breakpoints from the most common species in a

genus for the rarer ones is clinically safe. With the caveat that some species were only represented with few strains, azole and amphotericin B MICs above the wild-type range for *A. fumigatus* were observed for *A. ardalensis* (all azoles and amphotericin B), *A. micronesiensis* (posaconazole and isavuconazole), *A. polyporicola* (posaconazole, voriconazole and isavuconazole), *A. spelaeus* (posaconazole, voriconazole, isavuconazole and amphotericin B), *A. iizukae* (isavuconazole and amphotericin B), and *A. flavipes* and *A. urmiensis* (amphotericin B) questioning the appropriateness of these drug bug combinations in clinical practice. In contrast, *A. lanuginosus, A. luppiae, A. movilensis, A. neoflavipes*, *A. olivimuriae*, and *A. suttoniae* were highly susceptible to amphotericin B and azoles. The MICs for the remaining species were comparable to those of *A. fumigatus* suggesting that these species are appropriate targets for the amphotericin B and azoles. Finally, terbinafine was active against all species except *A. alboviridis*.

TAXONOMY

Aspergillus alboluteus F. Sklenar, Jurjević, Ezekiel, Houbraken & Hubka, ***sp. nov.*** MycoBank MB 839382. Fig. 8.

Etymology: Named after white (sporulation) and yellow (clusters of Hülle cells) colours of the colonies on most media.

Typus: **USA**, Pennsylvania, Philadelphia, outdoor air, 2014, isolated by Ž. Jurjević (**holotype** PRM 952200, isotype PRM 952201, culture ex-type CBS 145855 = EMSL 2420 = CCF 5695 = IFM 66815).

Colony diam, 25 °C, 7 d (mm): CYA: 15–27; CZA: 10–20; MEA: 13–26; OA: 18–26; CY20S: 25–29.

Culture characteristics, 25 °C, 7 d: CYA: Colonies centrally raised; texture floccose; margin undulate to filiform; mycelial areas and sporulation white (#ffffff) to cream (#fffdd0) with icterine (#fcf75e) patches due to Hülle cell clumps; exudate absent; reverse centrally dark goldenrod (#b8860b) to light french beige (#c8ad7f), in margins dutch white (#f1ddb8). CZA: Colonies flat; texture floccose to granular; margin entire to delicately filiform; mycelial areas and sporulation white (#ffffff) with lemon yellow (#fff44f) patches due to Hülle cell clumps; exudate absent; reverse centrally flax (#eedc82), in margins naples yellow (#fada5e). MEA: Colonies slightly centrally raised; texture floccose to granular; margin entire to delicately filiform; mycelial areas and sporulation white (#ffffff) with lemon yellow (#fff44f) patches due to Hülle cell clumps; exudate absent; reverse centrally copper (#b87333) to saddle brown (#964b00), in margins bronze (#cd7f32). OA: Colonies flat to umbonate; texture granular; margin entire to delicately filiform; mycelial areas and sporulation white (#ffffff); exudate absent; reverse centrally khaki (#c3b091) to bone (#e3dac9) in margins. CY20S: Colonies flat to slightly centrally raised; texture floccose; margin slightly undulate to delicately filiform; mycelial areas linen (#faf0e6), sporulation white (#ffffff); exudate absent; reverse ecru (#c2b280).

Cardinal temperatures: *Aspergillus alboluteus* grows very restrictedly at 10 °C, and the optimum growth temperature is 30 °C. This species is able to grow at 37 °C but not at 40 °C (Fig. 7).

Micromorphology: *Ascomata* absent. *Hülle cells* present in strains CCF 5695 and CCF 4916 and absent in strains CCF 6201 and DTO 410-I8, elongated, branched, 20–30 µm long, forming yellow clumps. *Conidial heads* globose to radiate (remaining compact). *Stipes* smooth, brown (always hyaline under the vesicle), (500–)800–1 200(–2 000) × 4–7(–10) µm; *vesicles* hyaline, subglobose, (6–)9–17(–20) µm diam; *metulae* hyaline, cylindrical, 5–7 µm long, covering two thirds to entire surface of the vesicle; *phialides* hyaline, flask-shaped, 6–8 µm long. *Conidia* globose to subglobose, smooth, hyaline 2.5–3.5 (2.9 ± 0.1) × 2–2.5 (2.4 ± 0.1) µm. *Accessory conidia* absent or rare, globose to subglobose, on short, hyaline micro- to semi-macronematous conidiophores.

Distinguishing characters: *Aspergillus alboluteus* is most closely related to *A. inusitatus*, but the latter is strikingly different from all related species by its green colonies and higher maximum growth temperature (40 °C). Phylogenetically, the next closest clade consists of *A. alboviridis*, *A. lanuginosus* and *A. movilensis*. *Aspergillus alboluteus* is phenotypically most similar to *A. movilensis*, that has similar colonies and also produces Hülle cells and accessory conidia with analogous morphology. However, these two species can be differentiated based on their conidiophore stipe lengths, vesicle diameters and colony sizes at 10 and 37 °C. The conidiophore stipes of *A. movilensis* rarely exceeds 400 µm, while stipes of *A. alboluteus* are (500–)800–1200(–2 000) µm long. The diameter of vesicles of *A. movilensis* rarely exceeds 13 µm, (5–)9–13(–16) µm, while vesicles of *A. alboluteus* are frequently larger, (6–)9–17(–20) µm. The colony diameters at 10 and 37 °C (on MEA, 14 d) slightly differ between these two species: at 10 °C, the colonies of *A. movilensis* attained 7 mm on average (the whole range was 6–8 mm), while colonies of *A. alboluteus* attained only 2 mm on average (1–2 mm); at 37 °C, *A. alboluteus* attained 18 mm on average (10–23 mm), while those of *A. movilensis* only 11 mm on average (6–19 mm).

Aspergillus alboviridis J.P.Z. Siqueira, Gené, F. Sklenar & Hubka, ***sp. nov.*** MycoBank MB 821808. Fig. 9.

Etymology: Refers to the white and green colony colour.

Typus: **Spain**, Balearic Islands, Mallorca, Pollença, herbivore dung, 2016, isolated by J. Gené and J.P.Z. Siqueira (**holotype** CBS H-23128, isotype PRM 954607, culture ex-type CBS 142665 = FMR 15175 = CCF 6049 = IFM 66819).

Colony diam, 25 °C, 7 d (mm): CYA: 19–21; CZA: 9–10; MEA: 18–23; OA: 18–19; CY20S: 23–24.

Culture characteristics, 25 °C, 7 d: CYA: Colonies centrally raised; texture floccose; margin entire; sporulation centrally green sheen (#6eaea1) to white (#ffffff) in margins; large clear droplets of exudate on the colony surface; reverse centrally gold metallic (#d4af37) to flax (#eedc82) in margins. CZA: Colonies convex; texture floccose; margin slightly undulate; sporulation centrally pale spring bud (#ecebbd) to white (#ffffff) in margins with canary (#ffff9a) circle close to margin formed by Hülle cells; clear droplets of exudate on the colony surface; reverse centrally satin sheen gold (#ce9d41) to gold crayola (#e6be8a), in margins dutch white (#f1ddb8) to bone (#e3dac9). MEA: Colonies flat to umbonate; texture floccose; margin entire to filiform; sporulation

centrally cambridge blue (#a3c1ad) to white (#ffffff) in margins with canary (#ffff9a) circle close to margin formed by Hülle cells; exudate absent; reverse centrally saddle brown (#964b00) to ochre (#cc7722), in margins earth yellow (#e1a95f). OA: Colonies slightly umbonate; texture floccose to granular, margin entire to delicately filiform; sporulation cenrally middle blue green (#8dd9cc) to white (#ffffff); clear droplets of exudate on the surface in the colony center; reverse centrally liver chestnut (#987456) to satin sheen gold (#ce9d41), in margins flax (#eedc82). CY20S: Colonies centrally raised, wrinkled; texture centrally velutinous to floccose in margins due to conidial heads; margin slightly undulate to filiform; sporulation centrally polished pine (#5da493) to white (#ffffff) in margins; exudate absent; reverse centrally antique bronze (#665d1e) to vegas gold (#c5b358), in margins dutch white (#f1ddb8).

Cardinal temperatures: *Aspergillus alboviridis* grows restrictedly at 10 °C, and the optimum growth temperature is around 25–30 °C. This species is able to grow very restrictedly at 37 °C (Fig. 7).

Micromorphology: *Ascomata* absent. *Hülle cells* elongated, frequently curved and branched, 20–30 µm long, forming yellow clumps. *Conidial heads* globose to compactly columnar. *Stipes* smooth, hyaline or brown (always hyaline under the vesicle), 120–200(–550) × 4.5–6(–8) µm; *vesicles* hyaline, globose to subglobose, 12–16(–20) µm diam; *metulae* hyaline, cylindrical, 6–7(–9) µm long, covering three quarters to entire surface of the vesicle; *phialides* hyaline, flask-shaped, 6–7.5(–8.5) µm long. *Conidia* globose to subglobose, smooth, hyaline 2.5–3.5 (2.9 ± 0.1) × 2–3 (2.5 ± 0.1). *Accessory conidia* not observed.

Distinguishing characters: *Aspergillus alboviridis* is most closely related to *A. lanuginosus* and *A. movilensis*. The colony colour of *A. alboviridis* is on some media in shades of green, most prominently on CYA, but also on MEA, OA and CY20S. Green coloured sporulation is not observed in *A. lanuginosus* and *A. movilensis*. *Aspergillus alboviridis* produces Hülle cells unlike *A. lanuginosus*. In contrast to *A. movilensis*, production of accessory conidia was not observed in *A. alboviridis*.

Aspergillus inusitatus F. Sklenar, C. Silva Pereira, Houbraken & Hubka, ***sp. nov.*** MycoBank MB 839383. Fig. 10.

Etymology: Name refers to the strikingly different colony morphology in comparison with other members of section *Flavipedes*.

Typus: **Tunisia**, Ras Rajel, soil in oak forest, 2009, isolated by C. Silva Pereira (**holotype** PRM 954606, culture ex-type DTO 121-G5 = CBS 147044 = CCF 6552).

Colony diam, 25 °C, 7 d (mm): CYA: 22–23; CZA: 8–9; MEA: 17–19; OA: 17–18; CY20S: 25–26.

Culture characteristics, 25 °C, 7 d: CYA: Colonies flat, densely covered with exudate droplets; texture floccose; margin delicately undulate or delicately filiform; sporulation bottle green (#006a4e), in margins maximum blue green (#30bfbf) to white (#ffffff); large clear or golden brown (#996515) droplets of exudate on the entire surface of the colony, small clear droplets in margins; reverse centrally satin sheen gold (#cba135), in margins flax (#eedc82). CZA: Colonies umbonate with raised edge; texture floccose, cottony in central area; margin delicately undulate to filiform; sporulation middle blue green (#8dd9cc) to cadmium green (#006b3c) or white (#ffffff), canary (#ffff9a) ring at the colony edge formed by clumps of Hülle cells; exudate absent; reverse centrally olive green (#b5b35c), in margins vegas gold (#c5b358) to flax (#eedc82). MEA: Colonies centrally raised, richly permeated with clumps of Hülle cells; texture floccose; margin slightly undulate to delicately filiform; sporulation british racing green (#004225) to bottle green (#006a4e) to maximum blue green (#30bfbf) with clear boundaries between sectors, in margins middle blue green (#8dd9cc) to white (#ffffff), canary (#ffff9a) circle in the middle of the colony formed by Hülle cells; exudate absent; reverse centrally metallic sunburst (#9c7c38) to saddle brown (#964b00), in margins sage (#bcb88a). OA: Colonies centrally raised, densely covered with exudate droplets; texture floccose; margin entire to delicately filiform; sporulation cadmium green (#006b3c) to middle blue green (#8dd9cc), in margins deep jungle green (#004b49) to maximum blue green (#30bfbf) to white; clear droplets of exudate mainly in the colony center, scarcely on the edge; reverse centrally straw (#e4d96f) to artichoke (#8f9779), in margins sage (#bcb88a). CY20S: Colonies centrally raised; texture floccose with cottony patches; margin delicately undulate to delicately filiform; sporulation british racing green (#004225) to bottle green (#006a4e), in margins middle blue green (#8dd9cc) to white (#ffffff), canary (#ffff9a) circle close to the colony edge formed by Hülle cells; exudate absent; reverse centrally straw (#e4d96f) to vegas gold (#c5b358), in margins flax (#eedc82).

Cardinal temperatures: *Aspergillus inusitatus* grows at 15 °C but does not grow at 10 °C. The optimum growth temperature is 30–35 °C. This species is able to grow restrictedly at 40 °C but not at 42 °C (Fig. 7).

Micromorphology: *Ascomata* absent. *Hülle cells* elongated, frequently curved or branched, 20–30 µm long or subglobose to ovate, 9–12 × 8–10 µm, forming yellow clumps. *Conidial heads* compactly radiate. *Stipes* smooth, hyaline or dark brown (always hyaline under the vesicle), 250–600 × 5–6 µm; *vesicles* hyaline, subglobose to pyriform, 15–18 µm diam; *metulae* hyaline, cylindrical, 6.5–7.5 µm long, usually covering the entire surface of the vesicle; *phialides* hyaline, flask-shaped, 7.5–8.5 µm long. *Conidia* subglobose, echinulate, fern green (#4f7942), 3.5–4 (3.6 ± 0.2) × 3–3.5 (3.1 ± 0.2) µm. *Accessory conidia* not observed.

Distinguishing characters: *Aspergillus inusitatus* is most closely related to *A. alboluteus.* Phylogenetically, the next closest clade consists of *A. alboviridis*, *A. lanuginosus* and *A. movilensis*. *Aspergillus inusitatus* differs strikingly from all these species by its dark green colony colour. The optimum growth temperature of *A. alboluteus*, *A. alboviridis*, *A. lanuginosus* and *A. movilensis* is around 25–30 °C, while the optimum growth temperature of *A. inusitatus* is 30–35 °C. Unlike the four above-mentioned species, *A. inusitatus* is able to grow at 40 °C. Furthermore, unlike all other species in the section *Flavipedes*, *A. inusitatus* produces echinulate conidia.

Aspergillus lanuginosus F. Sklenar & Hubka, ***sp. nov.*** MycoBank MB 839384. Fig. 11.

Etymology: Refers to the relatively rich production of aerial mycelium making the colonies downy on some media.

Typus: Haiti, Fonds Parisien, soil, unknown year of collection, unknown isolator (holotype PRM 954608, isotype PRM 954609, culture ex-type NRRL 4610 = IMI 350352 = CCF 4551 = IFM 66818).

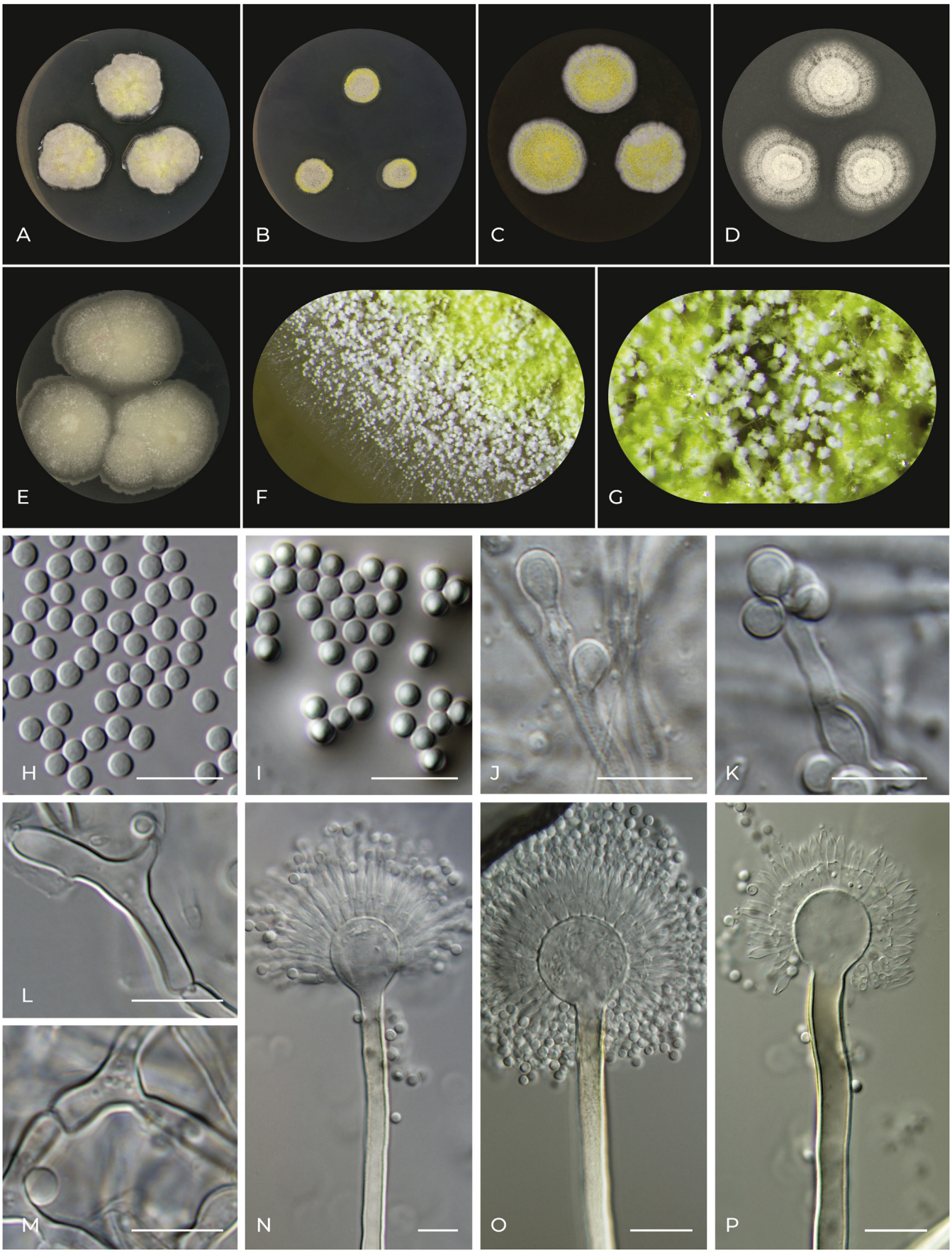

Fig. 8. Macromorphology and micromorphology of *Aspergillus alboluteus*. **A–E**. Colonies after 14 d at 25 °C, left to right: CYA, CZA, MEA, OA and CY20S. **F**. Detail of colony edge on MEA. **G**. Detail of conidial heads and Hülle cells on MEA. **H**. Conidia. **I**. Conidia in air bubble. **J**, **K**. Accessory conidia. **L**, **M**. Hülle cells. **N–P**. Conidiophores. Scale bars: H–P = 10 µm.

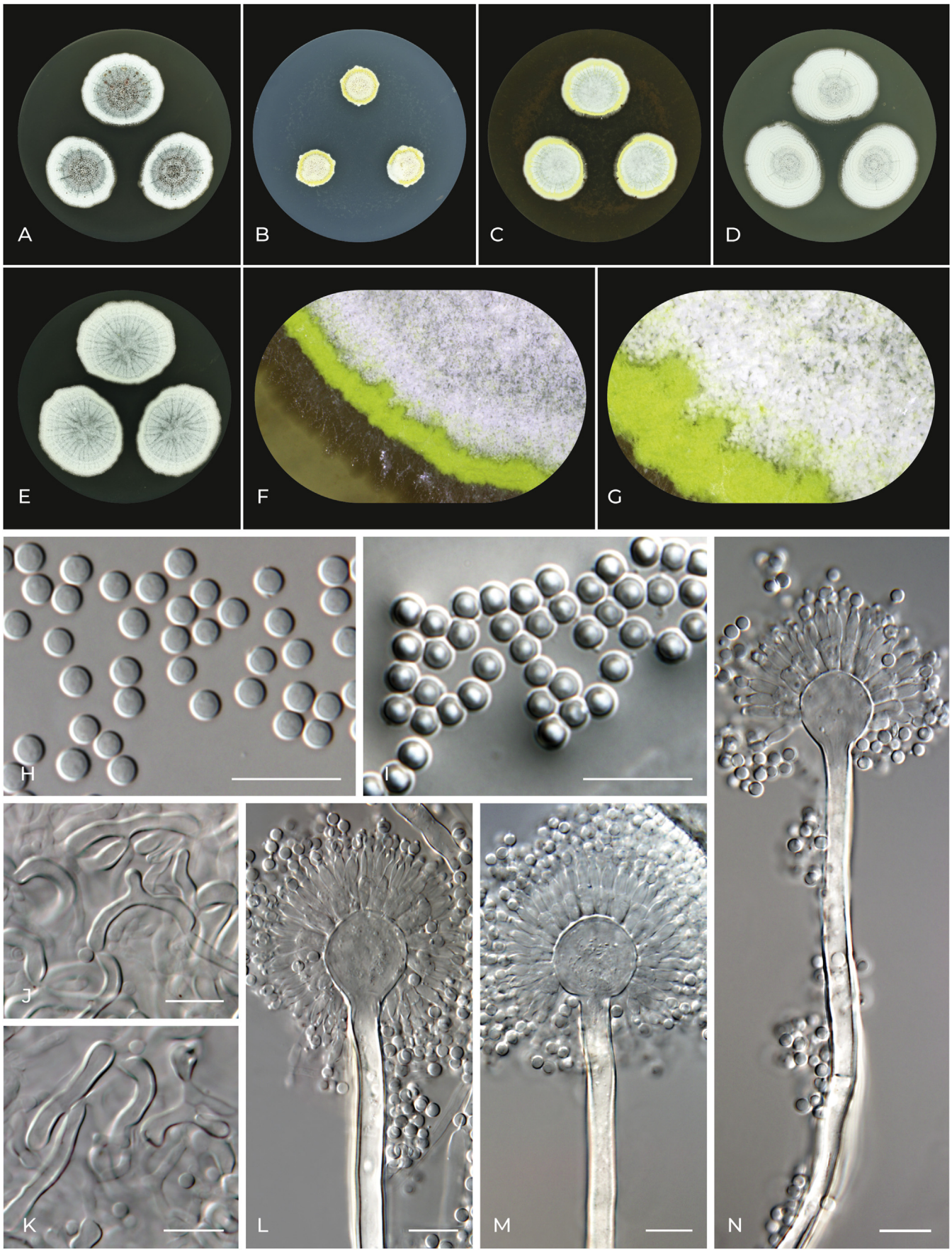

Fig. 9. Macromorphology and micromorphology of *Aspergillus alboviridis*. **A–E**. Colonies after 14 d at 25 °C, left to right: CYA, CZA, MEA, OA and CY20S. **F**, **G**. Detail of colony edge, conidial heads and Hülle cells on MEA. **H**. Conidia. **I**. Conidia in air bubble. **J**, **K**. Hülle cells. **L–N**. Conidiophores. Scale bars: H–N = 10 µm.

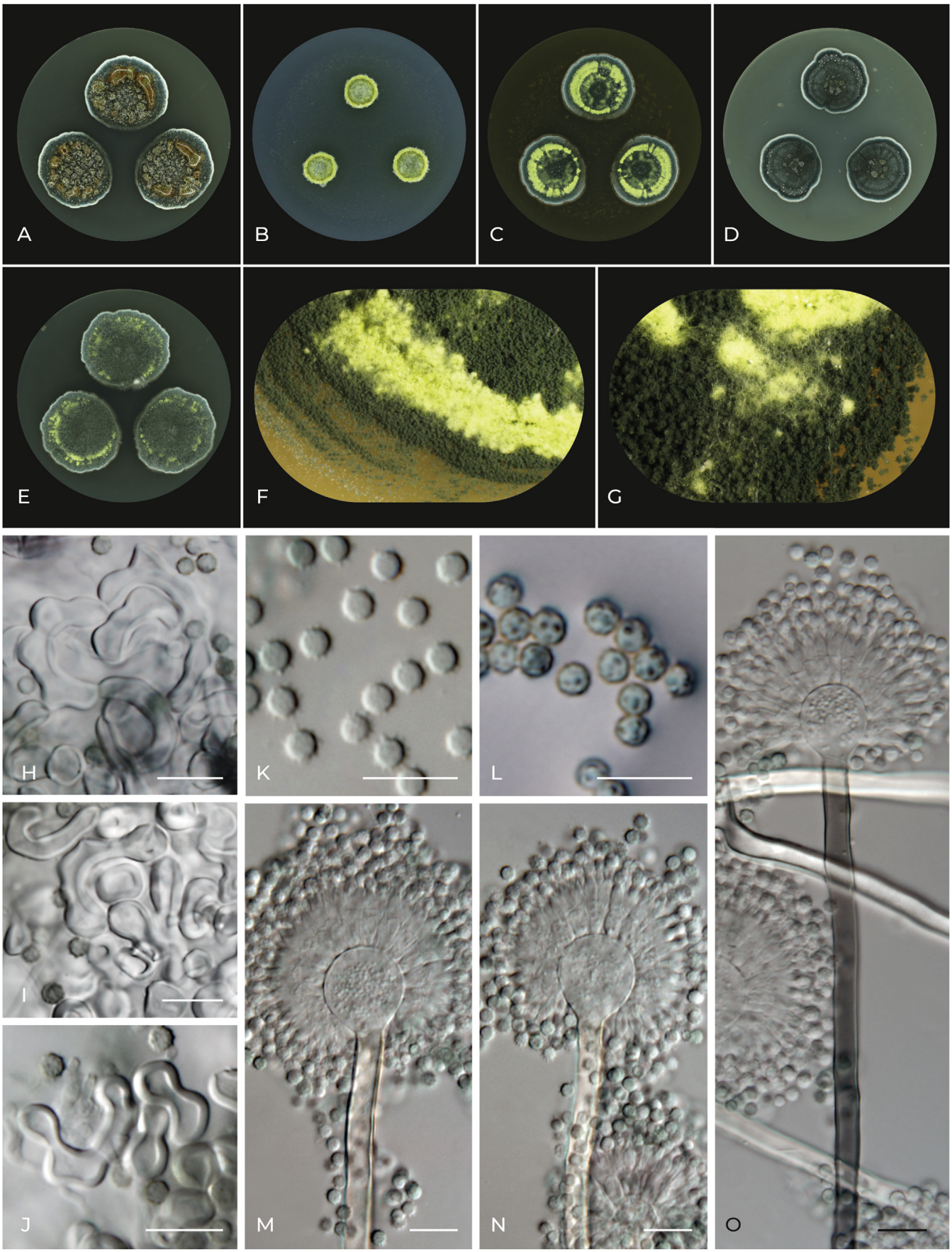

Fig. 10. Macromorphology and micromorphology of *Aspergillus inusitatus*. **A–E**. Colonies after 14 d at 25 °C, left to right: CYA, CZA, MEA, OA and CY20S. **F**. Detail of colony edge on MEA. **G**. Detail of conidial heads and Hülle cells on MEA. **H–J**. Hülle cells. **K**. Conidia. **L**. Conidia in air bubble. **M–O**. Conidiophores. Scale bars: H–O = 10 µm.

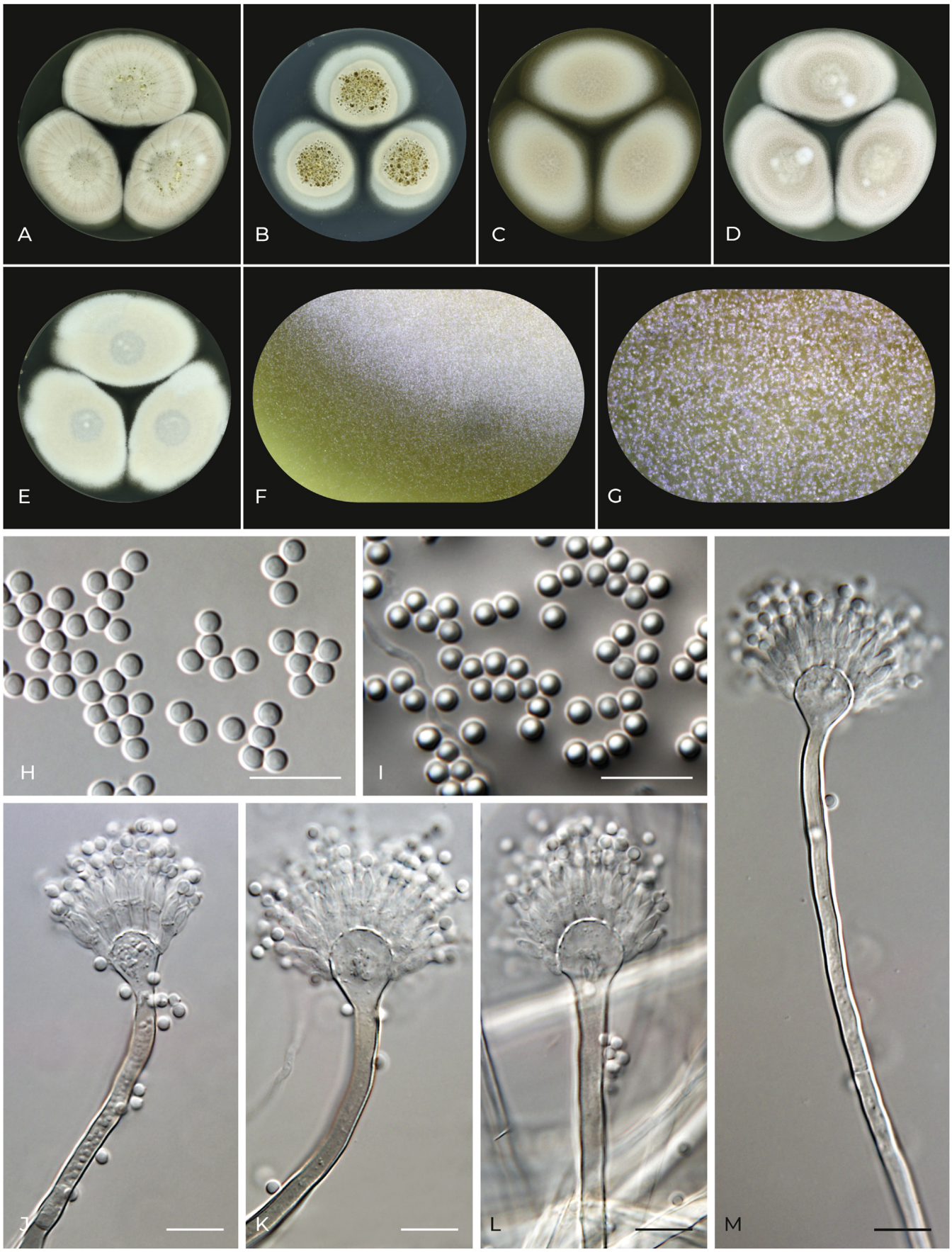

Fig. 11. Macromorphology and micromorphology of *Aspergillus lanuginosus*. **A–E**. Colonies after 14 d at 25 °C, left to right: CYA, CZA, MEA, OA and CY20S. **F**. Detail of colony edge on MEA. **G**. Detail of conidial heads on MEA. **H**. Conidia. **I**. Conidia in air bubble. **J–M**. Conidiophores. Scale bars: H–M = 10 µm.

Colony diam, 25 °C, 7 d (mm): CYA: 26–27; CZA: 21–22; MEA: 20–21; OA: 25–26; CY20S: 28–29.

Culture characteristics, 25 °C, 7 d: CYA: Colonies centrally raised; texture floccose; margin delicately filiform; sporulation centrally pale spring bud (#ecebbd) to beige (#f5f5dc) to champagne pink (#f1ddcf) in margins; clear droplets of exudate on the surface in the colony center; reverse centrally orange peel (ff9f00) to dutch white (f1ddb8) to gold crayola (e6be8a), in margins linen (#faf0e6). CZA: Colonies centrally raised; texture floccose; margin delicately filiform; sporulation centrally champagne pink (#f1ddcf), white (#ffffff) in margins; large amount of clear droplets of exudate on the surface in the colony center; reverse centrally camel (#c19a6b) to wheat (#f5deb3), in margins cream (#fffdd0). MEA: Colonies umbonate; texture cottony to floccose; margin delicately filiform; sporulation centrally champagne pink (#f1ddcf) to white (#ffffff) in margins; exudate absent; reverse centrally golden brown (#996515) to dark goldenrod (#b8860b), in margins maize crayola (#f2c649). OA: Colonies umbonate; texture floccose, cottony in the center; margin delicately filiform; sporulation centrally champagne pink (#f1ddcf) to white (#ffffff) in margins; exudate absent; reverse centrally antique bronze (#665d1e) to bistre brown (#967117), in margins flax (#eedc82). CY20S: Colonies flat to umbonate; texture floccose with small cottony patches in central areas; margin delicately filiform; sporulation centrally opal (#aac4c4) to linen (#faf0e6), in margins white (#ffffff); exudate absent; reverse centrally vegas gold (#c5b358) to bistre brown (#967117), in margins medium champagne (#f3e5ab).

Cardinal temperatures: *Aspergillus lanuginosus* grows at 10 °C, and the optimum growth temperature is 30 °C. This species is able to grow restrictedly at 37 °C but not at 40 °C (Fig. 7).

Micromorphology: *Ascomata* absent. *Hülle cells* absent. *Conidial heads* globose to radiate (remaining compact). *Stipes* smooth, hyaline or light brown (always hyaline under the vesicle), 600–1 100 × 3.5–4.5 µm; *vesicles* hyaline, subglobose to pyriform, 10–12 µm diam; *metulae* hyaline, cylindrical, 5–5.5 µm long, covering two thirds of the vesicle; *phialides* hyaline, flask-shaped, 5.5–6.5 µm long. *Conidia* globose to subglobose, smooth, hyaline 2.5–3 (2.7 ± 0.1) × 2–2.5 (2.3 ± 0.1) µm. *Accessory conidia* not observed.

Distinguishing characters: *Aspergillus lanuginosus* is most closely related to *A. alboviridis* and *A. movilensis*. In contrast to these two species, *A. lanuginosus* does not produce Hülle cells, its stipes are longer (*A. lanuginosus* 600–1 100 µm, *A. alboviridis* usually <200 µm, *A. movilensis* usually <400 µm) and the colony texture of *A. lanuginosus* on some media (MEA, OA, CY20S) is cottony, at least in the colony center, unlike the other species with mostly floccose colony texture.

Notes: The ex-type strain of *A. lanuginosus* NRRL 4610 was treated as *A. carneus* (section *Terrei*) by Raper & Fennell (1965). The phenotypic differences between ex-type strains of *A. movilensis* and *A. lanuginosus* were also observed by Hubka *et al.* (2015) who provisionally treated both strains as *A. movilensis*. These two strains (NRRL 4610 and NRRL 62819) also showed unique PCR fingerprinting pattern using the phage M13-core oligonucleotide primer and primer 834t (Hubka *et al.* 2015).

Aspergillus iizukae Sugiy., J. Fac. Sci. Univ. Tokyo, Sect. 3, Bot. 9: 390. 1967. MycoBank MB 326636.
Synonym: *Aspergillus capensis* Visagie *et al.*, Stud. Mycol. 78: 105. 2014. MycoBank MB 809193.

DISCUSSION

Species delimitation

In this study, we followed up on previous studies dealing with species delimitation in the genus *Aspergillus* (Sklenář *et al.* 2017, 2020, Hubka *et al.* 2018a, 2018b). The species delimitation step employing four single-locus and one multi-locus method was performed in the same way as in Sklenář *et al.* (2020). In contrast to our previous studies, here we presented the results of STACEY in the form of similarity matrices showing the assignments of individuals into species using several different values of the *collapseheight* parameter. This parameter is critical for the delimitation and its value is chosen arbitrarily. Our goal was to find the lowest value of the parameter which correctly delimits the species with indisputable species boundaries. These "reference species" differ from their close relatives clearly by phenotypic characters and/or were conclusively delimited by vast majority of single-locus delimitation methods. In the series *Flavipedes*, we considered *A. ardalensis*, *A. flavipes*, *A. suttoniae*, *A. templicola*, and *A. urmiensis* as these "reference species". The results of species delimitation methods in series *Spelaei* were less stable and only *A. luppiae* and *A. inusitatus* were regarded as "reference species". Then we checked how the results changed depending on the increase or decrease of the *collapseheight* parameter. For series *Flavipedes*, we concluded that a sensible value is 1×10^{-3}. Using this value, all currently known species except *A. capensis* were supported, with *A. templicola* having some probability of splitting into two species (Fig. 3A). A higher value of the *collapseheight* parameter (5×10^{-3}) resulted in excessive lumping, supporting only four species in the series (Supplementary Fig. S1A). When we used a lower value (1×10^{-4}), *A. templicola* and *A. micronesiensis* were split into several species, but *A. capensis* still formed one species together with strains of *A. iizukae* (Supplementary Fig. S1B).

The same value of the *collapseheight* parameter (1×10^{-3}) was applied on the series *Spelaei*. Using this value, STACEY supported all species related to *A. movilensis*, *i.e.*, *A. alboviridis*, *A. lanuginosus*, *A. movilensis*, *A. inusitatus* and *A. alboluteus* (Fig. 3B). All species were also delimited when a slightly lower value (7.5×10^{-4}) was used, but at the same time this value resulted in increased support for additional splitting of *A. polyporicola* and *A. spelaeus* (Supplementary Fig. S2B). On the other hand, slightly higher value (2×10^{-3}) resulted in lumping of *A. alboluteus* with *A. inusitatus*, and lower support for delimitation of *A. movilensis*/*A. alboviridis*/*A. lanuginosus*, and also *A. polyporicola*/*A. spelaeus* as separate species (Supplementary Fig. S2A).

The four single-locus methods gave mostly similar results within the series *Flavipedes*. The incongruences in the results were present among strains of *A. iizukae* and *A. capensis*, which are morphologically indistinguishable and the latter was described solely based on phylogeny (Visagie *et al.* 2014). Especially the results of single-locus delimitation methods based on the *benA* gene together with STACEY results indicate that recombination is present in this clade. This fact is also evident in the single gene phylogenies (Fig. 2) proving that recognition of *A. capensis* is not supported by genealogical concordance phylogenetic species recognition concept (GCPSR) (Taylor *et al.* 2000).

The results of single-locus methods within series *Spelaei* were more variable. The clade consisting of *A. spelaeus* and *A. polyporicola* was delimited as one species by 5/12 methods,

as two separate species by 5/12 methods, and as three species by 2/12 methods (Fig. 1B). *Aspergillus movilensis* clade consisting of *A. alboviridis*, *A. lanuginosus*, *A. movilensis*, *A. inusitatus* and *A. alboluteus* was delimited as one species by 1/12 methods, two species by 7/12 methods, five species by 3/12 methods, and six species 1/12 methods. In this ambiguous situation, our conclusions were significantly influenced by the presence of species-specific characters. Most importantly, *A. inusitatus* was conspicuously different compared to all other species within the section (Fig. 7, Table 3) and was also considered one of the "reference species" for STACEY method. In all cases where *A. inusitatus* was delimited as separate species, *A. alboviridis* and *A. lanuginosus* gained support.

The GMYC method is sometimes considered prone to over-splitting (Lohse 2009, Talavera *et al.* 2013), but it did not over-split the datasets in our previous study on the section *Nidulantes* (Sklenář *et al.* 2020), neither the dataset in this study. The method delimiting the highest number of species was bPTP and the most conservative method (resulting in the lowest number of delimited species) was bGMYC.

Species validation

For the species validation step, we employed the program DELINEATE, which is used for the first time to delimit species within the fungal kingdom. Until now, the most commonly used software for species validation was BPP (Bayesian Phylogenetics and Phylogeography) (Yang 2015). In the past studies on *Aspergillus*, this method was not very useful for distinguishing between different hypotheses on species boundaries, because its results are usually very benevolent, supporting even more splits than proposed by species delimitation methods. This excessive acceptance of splitting scenarios was also noted in other organisms and described by Sukumaran & Knowles (2017), who proposed the usage of the protracted speciation model by software for species validation. DELINEATE is the first program to challenge BPP as a choice for species validation.

In this study, BPP was only used as a tool for dividing the individuals from a given dataset into populations (Supplementary Table S1). The starBEAST was then used to calculate the "species tree" based on the populations. Finally, DELINEATE separated the populations from this tree into species. In contrast to BPP, at least some populations in DELINEATE need to be assigned to species (ideally those whose classification into species is clear) and others are left open to be delimited which offers opportunities to test a number of hypotheses. The limiting factor of the method are high computational demands that increase significantly with the number of unassigned populations. At the same time, a high total number of populations (unassigned and assigned into species) does not hinder the DELINEATE computation, but it can cause problems in starBEAST during species tree calculation.

Similarly to STACEY, where we applied several values of the *collapseheight* parameter, we generated several different models to be tested with DELINEATE. The results were again more complex in the series *Spelaei*, where we tested 14 models compared to only four models in series *Flavipedes*. The analysis of the model with all species in *A. movilensis* clade unassigned was not computationally feasible. Therefore, we had to generate separate models with different parts of the clade being unassigned (Fig. 4B, Fig. 5). When we left *A. alboviridis*, *A. lanuginosus* and *A. inusitatus* unassigned, as a result, they were lumped with their sister species. When *A. inusitatus* was defined as a separate species, *A. alboviridis* and *A. lanuginosus* were also separated from *A. movilensis*. Analogously, when *A. alboviridis* and *A. lanuginosus* were designated as separate species, *A. inusitatus* was also separated from *A. alboluteus*. Both parts of the analysis showed mixed support for the delimitation of *A. inusitatus* as separate species. But if *A. inusitatus* was designated as separate species, *A. alboviridis* and *A. lanuginosus* were consistently delimited as separate species too.

In the series *Flavipedes*, we mainly focused on the validation of species limits in the clade containing *A. iizukae* and *A. capensis* (Fig. 4A, Fig. 5). The results of all models were consistent. *Aspergillus capensis* was always lumped together with *A. iizukae.* Therefore, we consider *A. capensis* as a synonym of *A. iizukae*. *Aspergillus templicola* and *A. micronesiensis* were always delimited in the same way as suggested by majority of the species delimitation methods.

Furthermore, seven models of the whole section were generated to be tested in DELINEATE (Fig. 5). The results were congruent with the analyses performed separately in both series with one exception. The fourth model lumped *A. inusitatus* with *A. alboluteus* even though *A. alboviridis* and *A. lanuginosus* were specified as separate species. Based on our study, DELINEATE proved to give more relevant results which were more in agreement with putative species delimited in the first step of analysis compared to very benevolent BPP.

Similarly to our previous studies, we could not fully comply with the assumption of the species delimitation methods, *i.e.* not including species without variability (singleton species). It is a common issue in this kind of analyses and it has been discussed before (Ahrens *et al.* 2016). Singleton species are frequently described within genus *Aspergillus* with the general idea of the endeavor to describe all discovered diversity. The possibility of the singleton species (*A. alboviridis*, *A. lanuginosus* and *A. inusitatus*) being part of other closely related species was tested, but the results supported the splitting scenarios.

In this study, we enriched the analyses by addition of new strains and thus variability, resulting in more robust and accurate knowledge of the species boundaries in comparison with the previous studies on the section *Flavipedes*. In general, the data supported currently known species and in one case demonstrated recombination leading to synonymization of *A. capensis* with *A. iizukae*. A similar case occurred for instance in *A. parafelis* and *A. pseudofelis* (section *Fumigati*) which were described based on several strains with very limited genetic variability (Sugui *et al.* 2014) and later put into synonymy with *A. felis* when higher number of strains was available for analyses (Hubka *et al.* 2018a). The support for delimitation of *A. polyporicola* and *A. spelaeus* as separate species was also ambiguous (Fig. 1B). These two species were proposed by Hubka *et al.* (2015) based on the differences in their ecology and massive production of accessory conidia by *A. polyporicola* in contrast to *A. spelaeus.* In this study, we obtained new strains demonstrating that the ecological factor is not relevant as a taxonomic character for *A. polyporicola*, which was considered by Hubka *et al.* (2015) as a fungicolous species. We also examined the presence and abundance of accessory conidia in a broader set of *A. spelaeus* and *A. polyporicola* strains and we did not find any relevant differences between these two species – accessory conidia were rather rare or absent in all newly examined strains. *Aspergillus polyporicola* and *A. spelaeus* can be therefore considered cryptic species and there is a significant chance for their synonymization in the future when a larger

dataset will be available in terms of the number of strains or loci. But in the present study, the splitting scenario gained overall higher support. There is also no conflict in the topology of single-gene phylogenies and both species are supported by GCPSR (data not shown).

Incorporating multispecies coalescent model-based methods into taxonomy of *Aspergillus*

The polyphasic approach is currently a standard for species delimitation in *Aspergillus*. It always involves the assessment of phylogenetic data, with the GCPSR most commonly claimed to be used as a method of choice for delineation of species boundaries. It is however seldomly used methodologically properly as originally described by Dettman *et al.* (2003). Using the methods employed in this study, the final decision regarding the species boundaries remains partly subjective as other components of the polyphasic approach are still included in the decision-making process. The species delimitation part based on molecular data is however largely free from subjectivity and the methods force the taxonomists to take a fresh and unbiased look at the species limits. Furthermore, these coalescent-based methods are at least to some degree able to accommodate phenomena such as incomplete lineage sorting, recombination, or non-reciprocal monophyly (Edwards 2009). We do not expect or encourage these methods to replace the polyphasic approach, but they should enhance and strengthen it.

Several studies including this study highlighted the fact that the intraspecific genetic variability in *Aspergillus* is probably higher than expected and that species range sizes are unequal across aspergilli (Geiser *et al.* 2007, Hubka *et al.* 2018a). Consequently, it can be expected that the species numbers in some extensively studied groups with a narrow species concept will be reduced in the future. The resulting taxonomy should become clearer, which is demanded by user community given the number of studies (from clinical, biotechnological, or industrial background) struggling with the identification of cryptic *Aspergillus* species in the various species complexes (Negri *et al.* 2014, Pantelides *et al.* 2017, D'hooge *et al.* 2019, Imbert *et al.* 2019, Mincuzzi *et al.* 2020).

The ultimate future goal is to bring the majority of species in *Aspergillus* to the same level from the population genetics standpoint, which will certainly result in a delimitation of new species and synonymization of some others, with the synonymization being more likely in species groups which have been extensively studied and have a narrower species concept. An important prerequisite for these steps is a shift of taxonomy from a discovery phase, where species are described based on a small number of strains, to a phase where species limits are assessed based on large numbers of strains from different localities. It is already possible to obtain comprehensive datasets from databases for some species or species groups such as *A. fumigatus*, series *Nigri*, *Versicolores*, *Flavi* or others which can be re-analyzed using similar approaches.

Another important factor relevant for species concept in *Aspergillus* is the inevitable advent of species delimitation based on whole-genome sequences (Matute & Sepúlveda 2019). In this aspect, it is crucial not to exploit this vast source of genetic variability to flood the genus with cryptic species most likely corresponding to natural populations of a broader species, but to utilize it to learn more about the mechanisms of species boundaries formation and preservation, eventually leading to the establishment of meaningful rules for species delimitation (biologically meaningful species concept).

Ecology and clinical relevance

The ecology and clinical relevance of section *Flavipedes* members has been extensively reviewed by Hubka *et al.* (2015). The members of the section are distributed worldwide in soil, especially in tropical and subtropical regions (Klich 2002, Domsch *et al.* 2007, Choochuay *et al.* 2017). Some representatives are osmotolerant and xerophilic and they are frequently isolated from arid or saline environments, *e.g.* sea sand (Lee *et al.* 2016), saline soil (Kang *et al.* 2018) or salterns (Chung *et al.* 2019). There are also several reports on species adopting life strategy of plant endophytes (Luyen *et al.* 2019, Qin *et al.* 2019, El-Hawary *et al.* 2020). Other studies report another type of symbiosis of these fungi, namely with marine animals, sea cucumbers (Nerva *et al.* 2019) and marine sponges (Wiese *et al.* 2011). The same authors, Nerva *et al.* (2019), also reported that *A. spelaeus* harbors mycovirus Aspergillus spelaeus polymycovirus 1 (AsPMV1). Another habitat where section *Flavipedes* members are present is the cave environment. Numerous *A. spelaeus* strains used in this study originated from cave air or sediment and there are also reports of *A. iizukae* and *A. movilensis* isolated from caves (Hubka *et al.* 2015, Nováková *et al.* 2018). Similarly to many other Aspergilli, species from section *Flavipedes* spoil various food and feed (Pitt & Hocking 2009) and are frequently isolated from the indoor environment (Visagie *et al.* 2014, Sánchez Espinosa *et al.* 2021, this study). Even though hospitals can be also considered indoor environments, we highlighted these strains separately in Fig. 6, because some species have the potential to be pathogenic and hospital environment monitoring has usually a different purpose than monitoring indoor fungi in other buildings.

Some section *Flavipedes* members are uncommon human and animal pathogens. The majority of well documented cases of aspergillosis were attributed to *A. flavipes* and comprise diverse clinical manifestation including cutaneous aspergillosis (Barson & Ruymann 1986), onychomycosis (Gehlot *et al.* 2011), otomycosis (Stuart & Blank 1955), osteomyelitis (Roselle & Baird 1979), diskospondylitis (Schultz *et al.* 2008), pulmonary aspergillosis (Katou *et al.* 1999) and cerebral aspergillosis (Masih *et al.* 2016). However, the species identification of these strains according to the current taxonomy is mostly unclear except for the isolate associated with onychomycosis (GenBank EU515154) which represents *A. micronesiensis*. Even though there are sequences available for the strain VPCI 631/P/15 (GenBank KX455808, KX455766), a cause of cerebral aspergillosis (Masih *et al.* 2016), their information is contradictory. The *benA* sequences represent *A. flavipes s. str.*, while the *CaM* sequence represents *A. micronesiensis*. These two species are phylogenetically distant (Fig. 6) and one of these sequences was therefore most likely incorrectly deposited. Apart from mentioned cases, *A. micronesiensis* was also reported by Siqueira *et al.* (2018) from canine urine sample. The same authors also reported *A. iizukae* and *A. suttoniae* from human sputum and bronchoalveolar lavage, respectively, and *A. spelaeus* from human forearm. However, detailed information about clinical

relevance of these isolates was not included. In this study, we examined two strains (IHEM 22505 and IHEM 22506) originally identified as *A. flavipes* from human sputum and lung, respectively, which were reidentified as *A. micronesiensis*. Both strains were isolated from patients in Belgium and preserved in BCCM/IHEM collection. Another clinical strain examined here was obtained from bronchoalveolar lavage of a Danish patient and was identified as *A. templicola*. The available anamnestic data for these cases are limited and do not allow confirmation of the etiological relevance of strains.

The antifungal susceptibility patterns in section *Flavipedes* are largely unknown and restricted to few clinical isolates without clear species identification (*A. flavipes s. l.*) and examined by various methods (Del Carmen Serrano *et al.* 2003, Martin-Mazuelos *et al.* 2003, Masih *et al.* 2016). In this study, we evaluated antifungal susceptibilities to six antifungal agents in a large set of reliably identified strains across section *Flavipedes*. Our results showed notable differences in susceptibility pattern between the species as the MIC distributions for itraconazole, posaconazole, and isavuconazole spanned six two-fold dilutions and those for amphotericin B, voriconazole and terbinafine spanned seven two-fold dilutions across the 67 strains. In general, species-specific MIC distributions for wild type strains span three two-fold dilutions when tested in a single laboratory with a single batch of plates. Therefore, the difference in susceptibility among the species included herein cannot be explained by inherent variation of the test but must reflect intrinsic differences in susceptibility among the members of the *Aspergillus* section *Flavipedes*. About half of the species were susceptible to all agents whereas the remaining species were resistant to one or several agents. Therefore, species identification and susceptibility testing is important in clinical infections.

CONCLUSIONS

The revision of section *Flavipedes* led to an increase of its known variability. We performed phylogenetic and phenotypic analyses utilizing strains from previous studies and newly isolated strains. As a result, four species were newly described and one species, *A. capensis*, was put in synonymy. So far, the species from the series have been known to produce white, yellow, and brown colonies. The newly described species extend this heterogeneity, namely, the *A. inusitatus* deviates significantly by its dark green colonies and also colonies of *A. alboviridis* are light green on some media. The species delimitation analysis performed here builds upon recent studies on the genus *Aspergillus* and expands the spectrum of methods in the species validation step. Antifungal susceptibility across species diversity of the section *Flavipedes* showed elevated MICs to amphotericin B or azole derivates in significant part of the tested species, especially in those that are potentially clinically relevant. This finding emphasizes the need for species identification and susceptibility testing in clinical strains.

ACKNOWLEDGEMENTS

The project was supported by Czech Ministry of Health (grant NU21-05-00681) and the Charles University Research Centre program no. 204069. František Sklenář was supported by the project of Charles University Grant Agency (GAUK 140520). We are grateful to Jan Karhan for the help with graphical adjustments of analysis outputs. We thank Milada Chudíčková and Lenka Zídková for their invaluable assistance in the laboratory. Vit Hubka is grateful for the support from the Japan Society for the Promotion of Science Postdoctoral Fellowships for Research in Japan (Standard). This study was partially supported by the Grant-in-aid for JSPS research fellow (No. 20F20772).

APPENDIX A. SUPPLEMENTARY DATA

Supplementary data to this article can be found online at https://doi.org/10.1016/j.simyco.2021.100120.

REFERENCES

Ahrens D, Fujisawa T, Krammer HJ, *et al.* (2016). Rarity and incomplete sampling in DNA-based species delimitation. *Systematic Biology* **65**: 478–494.

Al-Dhabaan FA (2021). Mycoremediation of crude oil contaminated soil by specific fungi isolated from Dhahran in Saudi Arabia. *Saudi Journal of Biological Sciences* **28**: 73–77.

Arendrup MC, Jørgensen KM, Hanemaaijer N, *et al.* (2021). ISO standard 20776-1 or serial 2-fold dilution for antifungal susceptibility plate preparation: that is the question! *Journal of Antimicrobial Chemotherapy* **76**: 1793–1799.

Arzanlou M, Samadi R, Frisvad JC, *et al.* (2016). Two novel *Aspergillus* species from hypersaline soils of The National Park of Lake Urmia, Iran. *Mycological Progress* **15**: 1081–1092.

Barson WJ, Ruymann FB (1986). Palmar aspergillosis in immunocompromised children. *Pediatric Infectious Disease* **5**: 264–268.

Bouckaert R, Heled J, Kuhnert D, *et al.* (2014). BEAST 2: a software platform for Bayesian evolutionary analysis. *PLoS Computational Biology* **10**: e1003537.

Carmen Serrano M Del, Valverde-Conde A, Chávez M, *et al.* (2003). In vitro activity of voriconazole, itraconazole, caspofungin, anidulafungin (VER002, LY303366) and amphotericin B against *Aspergillus* spp. *Diagnostic Microbiology and Infectious Disease* **45**: 131–135.

Chen AJ, Hubka V, Frisvad JC, *et al.* (2017). Polyphasic taxonomy of *Aspergillus* section *Aspergillus* (formerly *Eurotium*), and its occurrence in indoor environments and food. *Studies in Mycology* **88**: 37–135.

Choochuay J, Xu X, Rukachaisirikul V, *et al.* (2017). Curvularin derivatives from the soil-derived fungus *Aspergillus polyporicola* PSU-RSPG187. *Phytochemistry Letters* **22**: 122–127.

Chung D, Kim H, Choi HS (2019). Fungi in salterns. *Journal of Microbiology* **57**: 717–724.

Crognale S, Pesciaroli L, Felli M, *et al.* (2019). *Aspergillus olivimuriae sp. nov.*, a halotolerant species isolated from olive brine. *International Journal of Systematic and Evolutionary Microbiology* **69**: 2899–2906.

Crous PW, Gams W, Stalpers JA, *et al.* (2004). MycoBank: an online initiative to launch mycology into the 21st century. *Studies in Mycology* **50**: 19–22.

Dettman JR, Jacobson DJ, Taylor JW (2003). A multilocus genealogical approach to phylogenetic species recognition in the model eukaryote *Neurospora*. *Evolution* **57**: 2703–2720.

D'hooge E, Becker P, Stubbe D, *et al.* (2019). Black aspergilli: a remaining challenge in fungal taxonomy? *Medical Mycology* **57**: 773–780.

Domsch KH, Gams W, Anderson T-H (2007). *Compendium of soil fungi*. IHW-Verlag. Eching, Germany.

Edwards SV (2009). Is a new and general theory of molecular systematics emerging? *Evolution* **63**: 1–19.

El-Elimat T, Raja HA, Graf TN, *et al.* (2014). Flavonolignans from *Aspergillus iizukae*, a fungal endophyte of milk thistle (*Silybum marianum*). *Journal of Natural Products* **77**: 193–199.

El-Hawary SS, Moawad AS, Bahr HS, *et al.* (2020). Natural product diversity from the endophytic fungi of the genus *Aspergillus*. *RSC Advances* **10**: 22058–22079.

El-Sayed ASA, Ali GS (2020). *Aspergillus flavipes* is a novel efficient biocontrol agent of *Phytophthora parasitica*. *Biological Control* **140**: 104072.

Frisvad JC, Larsen TO (2015). Chemodiversity in the genus *Aspergillus*. *Applied Microbiology and Biotechnology* **99**: 7859–7877.

Fujisawa T, Barraclough TG (2013). Delimiting species using single-locus data and the Generalized Mixed Yule Coalescent (GMYC) approach: a revised method and evaluation on simulated datasets. *Systematic Biology* **62**: 707–724.

Gams W, Christensen M, Onions AHS, *et al.* (1985). Infrageneric taxa of *Aspergillus*. In: *Advances in Penicillium and Aspergillus Systematics* (Samson RA, Pitt JI, eds). Plenum Press, New York: 55–62.

Gehlot P, Purohit DK, Singh SK (2011). Molecular diagnostics of human pathogenic *Aspergillus* species. *Indian Journal of Biotechnology* **10**: 207–211.

Geiser DM, Klich MA, Frisvad JC, *et al*. (2007). The current status of species recognition and identification in *Aspergillus*. *Studies in Mycology* **59**: 1–10.
Glass NL, Donaldson GC (1995). Development of primer sets designed for use with the PCR to amplify conserved genes from filamentous ascomycetes. *Applied and Environmental Microbiology* **61**: 1323–1330.
Greenhill AR, Blaney BJ, Shipton WA, *et al*. (2008). Mycotoxins and toxigenic fungi in sago starch from Papua New Guinea. *Letters in Applied Microbiology* **47**: 342–347.
Hall TA (1999). *BioEdit: a user-friendly biological sequence alignment editor and analysis program for Windows 95/98/NT. Nucleic Acids Symposium Series*: 95–98.
Heled J, Drummond AJ (2010). Bayesian inference of species trees from multilocus data. *Molecular Biology and Evolution* **27**: 570–580.
Hong S-B, Cho H-S, Shin H-D, *et al*. (2006). Novel *Neosartorya* species isolated from soil in Korea. *International Journal of Systematic and Evolutionary Microbiology* **56**: 477–486.
Houbraken J, Kocsubé S, Visagie CM, *et al*. (2020). Classification of *Aspergillus, Penicillium, Talaromyces* and related genera (*Eurotiales*): An overview of families, genera, subgenera, sections, series and species. *Studies in Mycology* **95**: 5–169.
Hubka V, Barrs V, Dudová Z, *et al*. (2018a). Unravelling species boundaries in the *Aspergillus viridinutans* complex (section *Fumigati*): opportunistic human and animal pathogens capable of interspecific hybridization. *Persoonia* **41**: 142–174.
Hubka V, Kolařík M (2012). β-tubulin paralogue *tubC* is frequently misidentified as the *benA* gene in *Aspergillus* section *Nigri* taxonomy: primer specifity testing and taxonomical consequences. *Persoonia* **29**: 1–10.
Hubka V, Nováková A, Jurjević Ž, *et al*. (2018b). Polyphasic data support the splitting of *Aspergillus candidus* into two species; proposal of *A. dobrogensis sp. nov. International Journal of Systematic and Evolutionary Microbiology* **68**: 995–1011.
Hubka V, Nováková A, Kolařík M, *et al*. (2015). Revision of *Aspergillus* section *Flavipedes*: seven new species and proposal of section *Jani sect. nov. Mycologia* **107**: 169–208.
Imbert S, Normand AC, Gabriel F, *et al*. (2019). Multi-centric evaluation of the online MSI platform for the identification of cryptic and rare species of *Aspergillus* by MALDI-TOF. *Medical Mycology* **57**: 962–968.
Jones G (2017). Algorithmic improvements to species delimitation and phylogeny estimation under the multispecies coalescent. *Journal of Mathematical Biology* **74**: 447–467.
Jurjević Ž, Kubátová A, Kolařík M, *et al*. (2015). Taxonomy of *Aspergillus* section *Petersonii sect. nov.* encompassing indoor and soil-borne species with predominant tropical distribution. *Plant Systematics and Evolution* **301**: 2441–2462.
Kang H-H, Zhang H-B, Zhong M-J, *et al*. (2018). Potential antiviral xanthones from a coastal saline soil fungus *Aspergillus iizukae*. *Marine Drugs* **16**: 449.
Katoh K, Standley DM (2013). MAFFT multiple sequence alignment software version 7: improvements in performance and usability. *Molecular Biology and Evolution* **30**: 772–780.
Katou K, Nanjou K, Kawakami M (1999). A case of chronic necrotizing pulmonary aspergillosis due to *Aspergillus flavipes* associated with pulmonary fibrosis. *Journal of the Japanese Respiratory Society* **37**: 938–942.
Klich MA (2002). Biogeography of *Aspergillus* species in soil and litter. *Mycologia* **94**: 21–27.
Kocsubé S, Perrone G, Magistà D, *et al*. (2016). *Aspergillus* is monophyletic: evidence from multiple gene phylogenies and extrolites profiles. *Studies in Mycology* **85**: 199–213.
Lee S, Park MS, Lim YW (2016). Diversity of marine-derived *Aspergillus* from tidal mudflats and sea sand in Korea. *Mycobiology* **44**: 237–247.
Letunic I, Bork P (2016). Interactive tree of life (iTOL) v3: an online tool for the display and annotation of phylogenetic and other trees. *Nucleic Acids Research* **44**: W242–W245.
Liu YJ, Whelen S, Hall BD (1999). Phylogenetic relationships among ascomycetes: evidence from an RNA polymerse II subunit. *Molecular Biology and Evolution* **16**: 1799–1808.
Lohse K (2009). Can mtDNA barcodes be used to delimit species? A response to Pons *et al*. (2006). *Systematic Biology* **58**: 439–442.
Luyen ND, Huong LM, Thi Hong Ha T, *et al*. (2019). Aspermicrones A-C, novel dibenzospiroketals from the seaweed-derived endophytic fungus *Aspergillus micronesiensis*. *Journal of Antibiotics* **72**: 843–847.
Martin-Mazuelos E, Pemán J, Valverde A, *et al*. (2003). Comparison of the Sensititre YeastOne colorimetric antifungal panel and Etest with the NCCLS M38-A method to determine the activity of amphotericin B and itraconazole against clinical isolates of *Aspergillus* spp. *Journal of Antimicrobial Chemotherapy* **52**: 365–370.
Masih A, Singh PK, Kathuria S, *et al*. (2016). Clinically significant rare *Aspergillus* species in a referral chest hospital, Delhi, India: molecular and MALDI TOF identification and their antifungal susceptibility profiles. *Journal of Clinical Microbiology* **54**: 2354–2364.
Matute DR, Sepúlveda VE (2019). Fungal species boundaries in the genomics era. *Fungal Genetics and Biology* **131**: 103249.
Mincuzzi A, Ippolito A, Montemurro C, *et al*. (2020). Characterization of *Penicillium s.s.* and *Aspergillus* sect. *Nigri* causing postharvest rots of pomegranate fruit in Southern Italy. *International Journal of Food Microbiology* **314**: 108389.
Negri C, Gonçalves S, Xafranski H, *et al*. (2014). Cryptic and rare *Aspergillus* species in Brazil: prevalence in clinical samples and *in vitro* susceptibility to triazoles. *Journal of Clinical Microbiology* **52**: 3633–3640.
Nerva L, Forgia M, Ciuffo M, *et al*. (2019). The mycovirome of a fungal collection from the sea cucumber *Holothuria polii*. *Virus Research* **273**: 197737.
Nguyen L-T, Schmidt HA, Haeseler A von, *et al*. (2015). IQ-TREE: a fast and effective stochastic algorithm for estimating maximum-likelihood phylogenies. *Molecular Biology and Evolution* **32**: 268–274.
Noman E, Al-Gheethi AA, Talip BA, *et al*. (2020). Oxidative enzymes from newly local strain *Aspergillus iizukae* EAN605 using pumpkin peels as a production substrate: optimized production, characterization, application and techno-economic analysis. *Journal of Hazardous Materials* **386**: 121954.
Nováková A, Hubka V, Valinová Š, *et al*. (2018). Cultivable microscopic fungi from an underground chemosynthesis-based ecosystem: a preliminary study. *Folia Microbiologica* **63**: 43–55.
O'Donnell K (1993). *Fusarium* and its near relatives. In: *The Fungal Holomorph: Mitotic, Meiotic and Pleomorphic Speciation in Fungal Systematics* (Reynolds DR, Taylor JW, eds). CAB International, Wallingford: 225–236.
O'Donnell K, Cigelnik E (1997). Two divergent intragenomic rDNA ITS2 types within a monophyletic lineage of the fungus *Fusarium* are nonorthologous. *Molecular Phylogenetics and Evolution* **7**: 103–116.
Pantelides IS, Aristeidou E, Lazari M, *et al*. (2017). Biodiversity and ochratoxin A profile of *Aspergillus* section *Nigri* populations isolated from wine grapes in Cyprus vineyards. *Food Microbiology* **67**: 106–115.
Paradis E (2010). pegas: an R package for population genetics with an integrated-modular approach. *Bioinformatics* **26**: 419–420.
Paradis E, Claude J, Strimmer K (2004). APE: analyses of phylogenetics and evolution in R language. *Bioinformatics* **20**: 289–290.
Peterson SW (2008). Phylogenetic analysis of *Aspergillus* species using DNA sequences from four loci. *Mycologia* **100**: 205–226.
Pitt JI, Hocking AD (2009). *Fungi and food spoilage*. Springer, London, UK.
Posada D (2008). jModelTest: phylogenetic model averaging. *Molecular Biology and Evolution* **25**: 1253–1256.
Qin J, Lyu A, Zhang Q, *et al*. (2019). Strain identification and metabolites isolation of *Aspergillus capensis* CanS-34A from *Brassica napus*. *Molecular Biology Reports* **46**: 3451–3460.
R Core Team (2015). *R: a language and environment for statistical computing*. R Foundation for Statistical Computing, Vienna, Austria.
Raper KB, Fennell DI (1965). *The genus Aspergillus*. Williams & Wilkins, Baltimore, MD, USA.
Reid NM, Carstens BC (2012). Phylogenetic estimation error can decrease the accuracy of species delimitation: a Bayesian implementation of the general mixed Yule-coalescent model. *BMC Evolutionary Biology* **12**: 196.
Ronquist F, Teslenko M, Mark P van der, *et al*. (2012). MrBayes 3.2: efficient Bayesian phylogenetic inference and model choice across a large model space. *Systematic Biology* **61**: 539–542.
Roselle GA, Baird IM (1979). *Aspergillus flavipes* group osteomyelitis. *Archives of Internal Medicine* **139**: 590–592.
Rossum G van, Drake FL (2019). *Python language reference, version 3*. Python Software Foundation.
Samson RA, Visagie CM, Houbraken J, *et al*. (2014). Phylogeny, identification and nomenclature of the genus *Aspergillus*. *Studies in Mycology* **78**: 141–173.
Sánchez Espinosa KC, Almaguer Chávez M, Duarte-Escalante E, *et al*. (2021). Phylogenetic identification, diversity, and richness of *Aspergillus* from homes in Havana, Cuba. *Microorganisms* **9**: 115.
Schultz RM, Johnson EG, Wisner ER, *et al*. (2008). Clinicopathologic and diagnostic imaging characteristics of systemic aspergillosis in 30 dogs. *Journal of Veterinary Internal Medicine* **22**: 851–859.

Siqueira JPZ, Wiederhold N, Gené J, *et al*. (2018). Cryptic *Aspergillus* from clinical samples in the USA and description of a new species in section *Flavipedes*. *Mycoses* **61**: 814–825.

Sklenář F, Ž Jurjević, Peterson SW, *et al*. (2020). Increasing the species diversity in the *Aspergillus* section *Nidulantes*: six novel species mainly from the indoor environment. *Mycologia* **112**: 342–370.

Sklenář F, Ž Jurjević, Zalar P, *et al*. (2017). Phylogeny of xerophilic aspergilli (subgenus *Aspergillus*) and taxonomic revision of section *Restricti*. *Studies in Mycology* **88**: 161–236.

Stuart EA, Blank F (1955). Aspergillosis of the ear; a report of twenty-nine cases. *Canadian Medical Association Journal* **72**: 334–337.

Sugui JA, Peterson SW, Figat A, *et al*. (2014). Genetic relatedness versus biological compatibility between *Aspergillus fumigatus* and related species. *Journal of Clinical Microbiology* **52**: 3707–3721.

Sukumaran J, Knowles LL (2017). Multispecies coalescent delimits structure, not species. *Proceedings of the National Academy of Sciences of the United States of America* **114**: 1607–1611.

Sukumaran J, Holder MT, Knowles LL (2021). Incorporating the speciation process into species delimitation. *PLoS Computational Biology* **17**: e1008924.

Talavera G, Dincă V, Vila R (2013). Factors affecting species delimitations with the GMYC model: insights from a butterfly survey. *Methods in Ecology and Evolution* **4**: 1101–1110.

Taylor JW, Jacobson DJ, Kroken S, *et al*. (2000). Phylogenetic species recognition and species concepts in fungi. *Fungal Genetics and Biology* **31**: 21–32.

Thom C, Church MB (1926). *The Aspergilli*. Williams & Wilkins, Baltimore, MD, USA.

Tuomi T, Reijula K, Johnsson T, *et al*. (2000). Mycotoxins in crude building materials from water-damaged buildings. *Applied and Environmental Microbiology* **66**: 1899–1904.

Valera HR, Gomes J, Lakshmi S, *et al*. (2005). Lovastatin production by solid state fermentation using *Aspergillus flavipes*. *Enzyme and Microbial Technology* **37**: 521–526.

Visagie CM, Hirooka Y, Tanney JB, *et al*. (2014). *Aspergillus, Penicillium* and *Talaromyces* isolated from house dust samples collected around the world. *Studies in Mycology* **78**: 63–139.

White TJ, Bruns TD, Lee SB, *et al*. (1990). Amplification and direct sequencing of ribosomal RNA genes and the internal transcribed spacer in fungi. In: *PCR–Protocols and Applications–a Laboratory Manual* (Innis M, Gelfand G, Sninsky J, White T, eds). Academic Press, San Diego: 315–322.

Wiese J, Ohlendorf B, Blümel M, *et al*. (2011). Phylogenetic identification of fungi isolated from the marine sponge *Tethya aurantium* and identification of their secondary metabolites. *Marine Drugs* **9**: 561–585.

Yang Z (2015). The BPP program for species tree estimation and species delimitation. *Current Zoology* **61**: 854–865.

Zhang J, Kapli P, Pavlidis P, *et al*. (2013). A general species delimitation method with applications to phylogenetic placements. *Bioinformatics* **29**: 2869–2876.

Zohri A-NA, Al-Bedak O (2020). *Aspergillus sakultaensis*, a new species in section *Flavipedes* isolated from Sohag Governorate, Egypt. *Journal of Environmental Studies* **20**: 21–27.